EVALUATION OF THE BLUESKY SMOKE FORECASTING SYSTEM AND ITS UTILITY FOR PUBLIC HEALTH PROTECTION IN BRITISH COLUMBIA

by

Jiayun Yao

B.Sc., Fudan University, 2010

A THESIS SUBMITTED IN PARTIAL FULFILLMENT OF

THE REQUIREMENTS FOR THE DEGREE OF

MASTER OF SCIENCE

in

THE FACULTY OF GRADUATE STUDIES

(Occupational and Environmental Hygiene)

THE UNIVERSITY OF BRITISH COLUMBIA

(Vancouver)

December 2012

Abstract

Wildfire smoke is a major contributor to extreme particulate matter (PM) air pollution events and has been associated with respiratory and cardiovascular health effects. With climate change, more frequent and intense wildfires are expected in the future and their impact on public health will likely increase. The existing exposure assessment tools such as the monitoring network and remote sensing platforms have limitations for measuring wildfire smoke, including inadequate coverage and measuring total column instead of ground-level concentrations. From the public health perspective, a system that can supplement these tools and predict smoke concentrations will be valuable. The Western Canada BlueSky Smoke Forecasting System, which can predict $PM_{2.5}$ (PM <2.5μm in diameter) from wildfires up to 60 hours in advance, has been developed since 2008. So far, there has not been any systematic and quantitative evaluation of its performance.

The first objective of this study was to evaluate the performance of BlueSky. We compared its forecasting output with monitoring measurements and remote sensing images with several different model evaluation statistics of temporal and spatial agreement. The second objective was to assess the association between BlueSky predictions and respiratory health indicators. Poisson regression was employed between BlueSky predictions and the health outcome indicators, including counts of prescriptions dispensed to relieve respiratory health symptoms and counts of physician visits for asthma.

Results suggested that BlueSky predicted smaller smoke plumes within the plumes observed by remote sensing. It predicted $PM_{2.5}$ concentrations comparable to monitor measurements in the middle of the fire period and in areas consistently impacted by wildfire smoke. More frequent and larger-scale overpredictions were observed.

A 30μg/m^3 increase in BlueSky 24-hour $PM_{2.5}$ predictions was associated with 1% increase in medication dispensations and physician visits for asthma. The relative risks were smaller than those associated with monitoring measurements. Smoke plume coverage predicted by BlueSky was associated with relative risks comparable with those observed by remote sensing.

In conclusion, BlueSky predictions were comparable with measurements from other smoke assessment tools and they were significantly associated with respiratory health outcomes. This study provides evidence to support the use of BlueSky in public health protection.

Preface

The Python codes and the R codes presented in Appendix A for BlueSky data preparation described in Section 2.1.1.1 were written by my thesis committee member Sarah Henderson.

Methods used in the evaluation of the BlueSky prediction model and the preliminary results were presented in a poster during the 21st Annual Meeting of the International Society of Exposure Science, Baltimore, Maryland, October 23 - 27, 2011. Similar materials were also presented orally at the 51st meeting of the Pacific Northwest International Section (PNWIS) of the Air and Waste Management Association in Harrison, British Columbia, November 8 – 11, 2011.

Summary of the BlueSky model evaluation results and preliminary results of the association between BlueSky predictions and health outcomes were shared in an article entitled: "Evaluation of the BlueSky Smoke Forecasting System and its utility for public health protection in BC" in the Canadian Smoke Newsletter.

Table of Contents

List of Tables

List of Figures

List of Abbreviations

AOD - aerosol optical depth

AQHI - air quality health index

BC - British Columbia

BCCDC - British Columbia Centre for Disease Control

BlueSky - BlueSky Western Canada Wildfire Smoke Forecasting System

CH_4 - methane

CI - confidence interval

CO - carbon monoxide

FAS - Fire Assimilation System

FB - fractional bias

FMS - figure of merit in space

FP - filter pressure

FRP - Fire Radiative Power

HMS - Hazard Mapping System

HYSPLIT - Hybrid Single-Particle Lagrangian Integrated Trajectory

IOA - index of agreement

km, km^2 - kilometer, square kilometer

LHA - local health area

MODIS - the Moderate Resolution Imaging Spectroradiometer

MSP - Medical Service Plan

NASA - National Aeronautics and Space Administration

NO, NO_x - nitrogen monoxide, nitrogen oxides

NOAA - National Oceanic and Atmospheric Administration

NRMSE - normalized root mean square error

O_3 - ozone

PAH - Polycyclic aromatic hydrocarbon

PM - particulate matter

PM_{10} - particulate matter with a diameter smaller than 10 micrometer

$PM_{2.5}$ - particulate matter with a diameter smaller than 2.5 micrometer

POM - particulate organic material

RR - relative risk

SFS - smoke forecasting system

SILAM - System for Integrated Modeling of Atmospheric Composition

SO_2 - sulfur dioxide

TA - Temperature Anomaly

$\mu g/m^3$ - microgram per cubic meter

Acknowledgements

First, I offer my heartfelt gratitude to my thesis committee for their guidance and expertise. My supervisor, Michael Brauer, has been supportive and helpful over the past two years and provided great ideas and suggestions for the thesis. Sarah Henderson, my committee member, has helped me out with many technical problems and constantly provided constructive feedback for my work. Ian Mckendry, another committee member of mine, has helped to build my basic knowledge of air quality modeling and provided useful advice on the thesis writing.

I wish to thank the experts who are involved in the development and maintenance of the BlueSky system for sharing their expertise. In particular, George Hicks, former staff in the Department of Earth, Ocean and Atmospheric Sciences, University of British Columbia, provided the BlueSky data and Steve Sakiyama at BC Ministry of Environment shared his insights for some of my study results.

I would also like to thank the group of Environmental Health Services at BCCDC for providing access to the health data.

Financial support for my training was generously provided by the Collaborative Research and Training Experience – Atmospheric Aerosol Program funded by Natural Sciences and Engineering Research Council of Canada. The project was financially supported by BC Clean Air Research Fund.

I'm grateful for the moral support from my friends near and far. Last but not least, I want to dedicate this work to my parents for their unconditional support throughout my years of education.

.

1. Introduction and literature review

1.1 Background

1.1.1 Introduction

Wildfire is a hazard for populations in many regions of the world. In Canada, about 40% of the country is covered by forests or other wooded land (Stocks et al., 2002), and approximately 2.5 million hectares are burned annually on average (Government of Canada, 2010). British Columbia (BC) is one region that is prone to extensive burning during the wildfire season, which varies from year to year depending on weather conditions, but generally starts in April and lasts until September. The forest fire season of 2010 was one of the worst on record, with the most area burnt in the past ten years and more than 200 reported fires involving areas 5 hectares and larger (BC Forest Service, 2011). More widespread, frequent and severe wildfires have occurred in North America during the last two decades, and this trend is anticipated to continue in the future along with climate change (Westerling et al., 2006; Flanigan and Van Wagner, 1991; Wotton et al., 2010).

While wildfires can be a direct threat to property and life in nearby populations, they can also impact on the health of populations in more extensive areas on a local, regional or even global scale through the transport of the wildfire smoke. Significant elevated concentrations of multiple air pollutants resulting from the emissions of fire smoke have been documented (Viswanathan et al., 2006; Phuleria et al., 2005; Keane, 2012). Many of these pollutants, such as particulate matter (PM) and carbon monoxide (CO), have been associated with adverse health effects. Among them, PM has been found the most elevated and the most persistently elevated during fire periods, even in areas at great distances from the fire locations.

Phuleria et al. (2005) found that PM_{10} (particulate matter with a diameter smaller than 10 micrometer) concentrations at Los Angeles during the massive wildfires in southern California in 2003 were 3 to 4 times higher than nonfire periods, while the concentrations of CO, nitrogen oxides (NO_x) and ozone (O_3) were increased by a factor smaller than 2, unchanged, or even reduced. In a study by Sapkota et al. (2005), as much as a 30-fold increase in ambient $PM_{2.5}$ (particulate matter with a diameter smaller than 2.5 micrometer) was recorded in Baltimore City, a place located thousands of kilometers away from the wildfire source in Quebec, Canada. In addition, $PM_{2.5}$ is one of the most widely monitored air pollutants, with well-established reports of its impacts on human health. These characteristics have made it the best exposure metric to access air quality and health impacts from wildfire smoke (Naeher et al., 2007).

Measurement tools to assess smoke exposure in Canada include $PM_{2.5}$ measurements from regulatory air monitoring networks and products generated from remote sensing data. These tools, however, have limitations. While wildfire smoke can impact large populations, the available monitoring networks may not provide adequate coverage for estimation of health impacts, and the instruments may fail during smoke events with extremely high concentrations. On the other hand, remote sensing data cover very large areas, but they represent the smoke in the total column of the atmosphere, which can be different from the ground-level conditions of most concern.

From the perspective of supporting public health actions to mitigate the health impacts from wildfire smoke, another important limitation of these tools is that they can only provide retrospective or near-real-time measurements, not prospective forecasts. Many other public health hazards are routinely forecast, including high temperature, ultraviolet exposure, and

pollen levels. Such forecasts allow extra time for public health practitioners to inform the public and take measures to help them mitigate the impacts, before the hazards actually take place. These publicly available forecasts can also allow the public to self-monitor, taking actions according to their own sensitivity to these hazards. As wildfire smoke is a short-term exposure with high concentrations, effective predictions will be invaluable for informing timely public health actions.

A need for a smoke forecasting system in Canada was identified in 2007, with one of the objectives to support public health decision making. The development of this new system, called the Western Canada BlueSky Smoke Forecasting System (BlueSky), was started in 2008. This forecasting approach can supplement real-time regulatory monitoring and remote sensing data and predict ground-level concentrations in advance.

So far, there has not been any quantitative and systematic evaluation of the system performance. This thesis research aims to fill this gap and to assess the utility of this new system for public health protection by (1) comparing BlueSky predictions with other measures of smoke, and (2) evaluating the association between BlueSky predictions with health outcome measurements.

1.1.2 Study area

Although the BlueSky prediction domain has now been expanded from the west coast to north-western Ontario, the scope of this study focuses only on its performance in the Province of BC. When the thesis was initiated, BlueSky only covered BC and Alberta, and BC had one of the most dense air quality monitoring networks in Canada, providing sufficient

data for the study. Moreover, in collaboration with BC Center for Disease Control (BCCDC), we were able to obtain health data within BC.

The total area of the province measures 944,735 square kilometers (km^2). About two-thirds of the province is covered by forests (BC Ministry of Forests, Mines and Lands, 2010) and an average of 985km^2 was burnt annually in the last decade.

1.1.3 Study period

In 2010, massive wildfire events started around July 28th when lightning storms hit the central interior where forest fuels had been dried by the hot sunshine for the whole July. In addition, forests in BC were widely attacked by mountain pine beetles in recent years, which largely increased the flammability of the fuels (Kurz et al., 2008; Page et al., 2012). Numerous fires rapidly burnt large areas of forest throughout, August with only a brief break in mid-August. Cooler temperatures and precipitation drew an end to this fire season at the end of August (Province of British Columbia, 2011). More than 330,000 hectares of forest were burned in BC in 2010 and the most severely impacted areas were in the central interior (Province of British Columbia, 2011). Figure 1.1 shows the locations of all fires and their sizes in BC during 2010.

Accordingly, analyses in this study focused on the 35-day period between July 24th and August 29th to capture the whole active fire season in 2010.

1.1.4 Study population and local health areas

The total population in BC was estimated to be 4,529,674 in 2010 (BC Stats, 2011). For the purposes of health administration, the smallest geographic units in BC are the 89 local

health areas (LHAs) (BC Stats, 2007). In this study, the LHA was used as the basic unit of aggregation for all health outcomes. The outcomes included daily counts of physician billings for asthma from the Medical Service Plan (MSP) database, and daily counts of pharmaceutical dispensations for salbutamol (an inhaled medication to relieve the symptoms of asthma) from the PharmaNet database. These outcomes were used to examine the association between exposure assessment tools and population health responses.

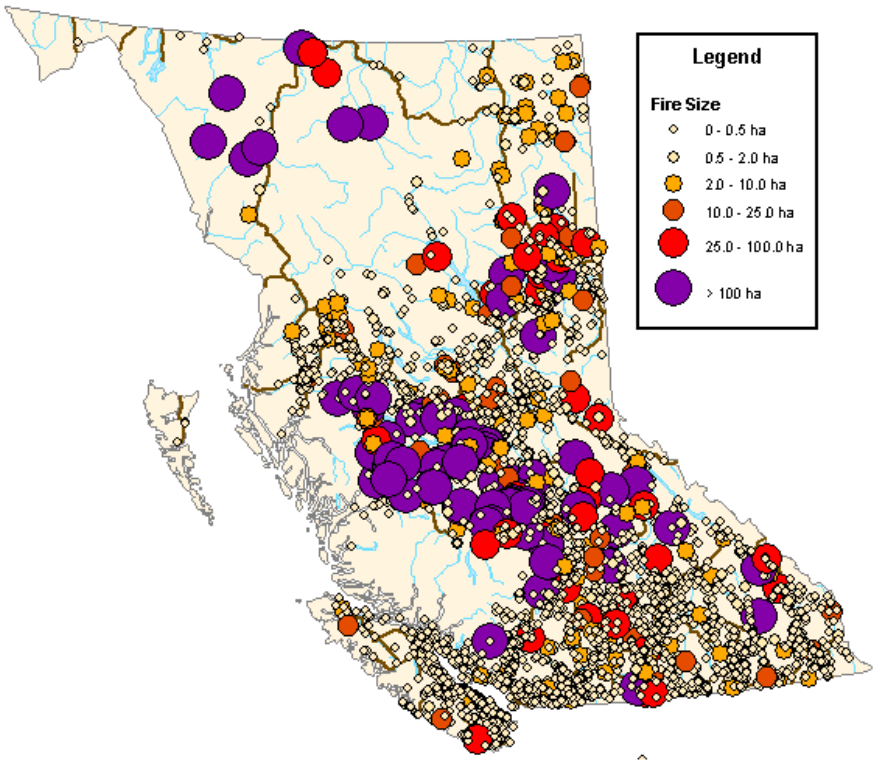

Figure 1.1 Locations of all wildfires in 2010 in British Columbia. (Province of British Columbia, 2011)

1.2 Rationale and objectives

1.2.1 Rationale

To evaluate the performance of a prediction model, observations from ground monitors and satellites can act as references against which to compare the forecasts. While air quality

monitoring stations can measure relatively accurate surface concentrations of $PM_{2.5}$, they are spatially sparse, with only 55 monitors to cover 944,735 km^2 during the study period. While remote sensing data can provide spatially extensive images of forest fire smoke, they reflect smoke in the total atmospheric column and not at the surface where people are exposed. By using both of these two tools as references, we can provide a more comprehensive assessment of the model performance. The better (1) the predicted $PM_{2.5}$ concentrations agree with the monitoring data, and (2) the smoke plume shapes agree with the remote sensing data, the better the model performs. Correlation and difference between predicted and observed values as well as spatial statistics comparing the intersection and union of the predicted and observed smoke plumes are indicators of the agreement.

Wildfire smoke is one of the major contributors to extreme particulate matter pollution events, and there is toxicological and epidemiological evidence supporting the link between wildfire smoke and cardio-respiratory health impacts (Andreae and Merlet, 2001; Migliaccio et al., 2010; Naeher et al., 2007). BlueSky, as a smoke forecasting system, provides advance predictions of wildfire smoke PM exposure levels. If there is an association between BlueSky predictions and health outcomes, such as MSP claims or pharmaceutical dispensations, it can support the feasibility of using BlueSky as an indicator of health impacts expected from the fire events, allowing public health authorities to prepare strategies in advance. In other words, different mitigation strategies, ranging from staying indoors and reducing activities to using air filter, to setting up clean air shelter, or even to evacuation, can be announced in advance corresponding to the exposure levels predicted by BlueSky, to reduce the public health effects associated with those exposure levels.

1.2.2 Objectives

The **first objective** is to evaluate the day-by-day performance of BlueSky in BC during the 2010 wildfire season (July 24th – August 29th, 2010), including the correlation and difference between BlueSky $PM_{2.5}$ predictions and monitoring $PM_{2.5}$ measurements (including the spatial agreement at fixed times and the temporal agreement at fixed locations) as well as the extent of overlap between BlueSky smoke plumes and HMS smoke plumes.

The **second objective** is to evaluate the association between BlueSky predictions ($PM_{2.5}$ concentrations and smoke plume coverage) and (1) the counts of MSP claims for respiratory illnesses and (2) dispensations of salbutamol (used to relieve acute symptoms of asthma) during wildfire periods.

1.3 Literature review

1.3.1 Physical, chemical and behavioral characteristics of wildfire smoke

Smoke emissions from wildfires include gases such as O_3, CO, CO_2, and NO_x. They also include solids in the form of PM of varying sizes and compositions. Andreae and Merlet (2001) summarized literature describing emission factors of major pollutants from biomass burning from non-tropical forest fires (Table 1.1). However, these emissions factors vary largely at different stages of the combustion process. During the flaming phase of combustion, when the temperature is high, major substances released include simple molecules such as CO_2, water, nitrogen monoxide (NO), and sulfur dioxide (SO_2) and intermediate products of flame radical chemistry such as methane (CH_4), polycyclic aromatic hydrocarbons (PAH) and soot particles (Andreae and Merlet, 2001). After the flaming phase, the combustion will begin a smoldering phase, which is a process of low temperature burning. During this phase,

incompletely combusted products like CO dominate the emissions (Andreae and Merlet, 2001). This great variability in composition of wildfire smoke contributes largely to the complexity in studying its impact on air quality and population health. Thus, it is vital to establish a good metric for exposure assessment.

According to a systematic review on biomass burning emissions by Reid et al. (2005), the majority of carbon content is released as CO_2 or CO and, typically, less than 5% is released as particulate matter. The particle formation process mainly occurs during flaming combustion, beginning with the creation of condensation nuclei such as PAH from the emitted gases, and growing through chemical and coagulative processes. During this process, increased fire intensity is shown to increase particle size and production because the intense flame reduces oxygen transport into the interior flame zone. The smoldering combustion phase produces extremely small amount of soot particles. However, relatively larger particles can be formed in this phase by condensation of volatilized organics on un-combusted particles (Reid et al., 2005).

Despite the fact that much less carbon is released as PM compared with gaseous emissions, PM has been identified as the best exposure metric for wildfire smoke because it tends to be the most elevated in ambient air among all of the regulatory air pollutants. In addition, fine particles can remain suspended in the air for long periods, thus allowing smoke to travel long distances between fire sites and human populations, impacting much larger population.

The most common measures of PM are the mass concentration of PM_{10} and $PM_{2.5}$. The measured daily maximum PM_{10} concentrations at locations influenced by wildfire events around the world have ranged up to between 60 and 850 $\mu g/m^3$ (Kochi et al., 2010). As formed by combustion, the size distribution of PM originated from wildfires peaks between

0.1 μm and 1 μm (Sillanpää et al., 2005; Samsonov et al., 2010; Pio et al., 2008). Laboratory examination of wood burning emissions shows similar results, with the peaks in mass concentration of particles with diameters of around 0.1 μm (Hueglin et al., 1997). These findings are consistent with the high $PM_{2.5}/PM_{10}$ mass ratios observed in several wildfire smoke studies (Moore et al., 2006, Wu et al. 2006). This is the result of the dominant formation process by condensation during flaming combustion.

Table 1.1 Emission factors for major pyrogenic species from fires in non-tropical forests. (Andreae and Merlet ,2001)

Species	Emissions factors (g/kg dry fuel)*	Species	Emissions factors (g/kg dry fuel)
CO	1569 ±131	NO_x	3.0 ±1.4
CO_2	107 ±37	$PM_{2.5}$	13.0 ±7.0
CH_4	4.7 ±1.9	TPM**	17.6 ±6.4

*Emissions factor is defined as the amount of a compound released per amount of dry fuel consumed.
**TPM: total particulate matter, airborne particulate matter with an upper size limit of approximately 100 μm in diameter

There are three principal components of PM from biomass burning: particulate organic material (POM), black carbon, and trace inorganic species (Reid et al., 2005). In fresh dry smoke particles, POM accounts for about 80% of the mass, followed by 5–9% for black carbon, and 12–15% for other trace inorganic species (Reid et al., 2005). Typical tracers regarded as indicators of biomass burning include levoglucosan, potassium, and oxalate (Pio et al., 2008; Okuda et al., 2002; Saarnio et al., 2010). While potassium and oxalate are plant nutrients themselves, levoglucosan is commonly formed from the thermochemical decomposition of carbohydrates in biomass, such as starch and cellulose (Lakshmanan & Hoelscher, 1970).

Compositions of PM vary by combustion efficiency and fuel type. Generally, particles from the flaming phase have more black carbon and less organic carbon than particles from the smoldering phase. Because the organic fraction of particles is mainly composed of unburned material or incomplete combustion products, the composition of this fraction is largely dependent on components of the fuel (Reid et al., 2005).

Wildfire smoke can be dispersed and transported on the regional, continental and intercontinental scale. Small scale fires may impact surrounding areas, communities or cities downwind, but smoke from large scale fires can be transported over vast distances. There have been reports on long-range transport of Canadian wildfire smoke to places as far as Greenland, the southeastern United States, and across the Atlantic Ocean to Europe (Hsu et al., 1999; Formenti et al., 2002; Fiebig et al., 2002; Wandinger et al., 2002; Wotawa & Trainer, 2000). With some even more extreme conditions, there have been hemispheric-scale transports of smoke from forest fires in Russia and Australia, which travelled around the world in about 15 days (Damoah et al., 2004; Dirksen et al., 2009). Generally, long-range transport can occur when (1) intense heat in the smoke plume results in smoke being injected high into the atmosphere, (2) strong convection from frontal or cyclone systems allow smoke plumes to be lofted to the upper troposphere or even the lower stratosphere, resulting in rapid transportation at high altitudes, and (3) rapid spread and persistent fires provide continuous sources of smoke emissions.

1.3.2 Health impacts of wildfire smoke

Wildfire smoke can contribute to extensive air quality degradation, and poor air quality is associated with many adverse human health effects. It follows that the public health im-

pacts from wildfire smoke have been widely studied, especially in the past decade.

A recent study estimates that 339,000 deaths can be attributed to landscape fire smoke exposure annually around the world and the most affected regions are Sub-Saharan Africa and Southeast Asia where landscape fires can last for months in a year (Johnston et al., 2012). In North America wildfires are mostly episodic, typically leading to very high smoke exposures over short periods. Many of the constituents of wildfire smoke have been extensively studied with respect to their adverse health effects. For example, CO is known to be highly toxic to humans and animals because it can combine with hemoglobin, leading to ineffectiveness for delivering oxygen to bodily tissues (Tikuisis et al., 1992). O_3, another pollutant from wildfire smoke, is a strong oxidant and can cause harm to lung function and the respiratory system. Exposure to ozone has been associated with premature death, asthma, bronchitis, heart attack, and other cardiopulmonary problems (Weinhold, 2008). However, these pollutants are relatively short-lived and their health impacts are largely constrained to people in direct contact with fires, such as firefighters and residents living very close to the fire source. In addition, the health effects of these single gases are expected to be the same, regardless of their source. Fine particulate matter ($PM_{2.5}$), on the other hand, can be suspended in the atmosphere for a long time and can be transported to large areas at great distances from a fire source. Its size distribution and composition can vary considerably from different sources, leading to potentially different health impacts. Thus, $PM_{2.5}$ is the biggest concern from the perspective of public health protection against wildfire smoke. Both toxicology experiments and epidemiologic studies have associated wildfire smoke particulate matter exposure with a range of health outcomes.

1.3.2.1 Toxicological studies on health effects of woodsmoke

The size fraction of PM is one of the influential factors on its toxicology. It has been demonstrated by *in vitro* toxicological studies that $PM_{2.5}$ induces stronger cytotoxicity, mutagenicity, DNA damage and stimulation of proinflammatory cytokine production than PM_{10}. This is mainly due to its deeper penetration into the lung and specific chemical compositions (De Kok et al., 2006). Thus, PM emitted from sources such as biomass burning and mobile vehicles, which have high $PM_{2.5}/PM_{10}$ ratios, may be more toxic than PM generated from sources such as dust storms with a larger fraction of coarse particles.

A review by Migliaccio et al. (2010) suggests that experimental studies involving different animal models have been conducted on the health concerns of episodic exposure to wood smoke. Health effects of concern include general irritation, exacerbation of existing cardiorespiratory conditions, and effects on immune system. Another review by Naeher et al. (2007) concludes that the available toxicological studies indicate exposure to wood smoke can significantly impact respiratory immune system, and can induce permanent impairment in lung tissues at high doses. At the same time, wood smoke is genotoxic and potentially carcinogenic.

While both wood smoke and traffic-related PM are released from combustion process and have similar size distributions, studies comparing the toxicity of the two have produced inconsistent results. Several studies have found more DNA damage and higher genotoxicity in wood smoke than in traffic-related PM (Danielsen et al. 2009; Forchhammer et al., 2012), possibly due to the higher concentrations of PAHs in wood smoke (Danielsen et al. 2009, Kocbach et al., 2008a; Samuelsen et al., 2008; Forchhammer et al., 2012). However, Karlsson et al. (2006) and Kubatova et al. (2004) have found similar or lower genotoxicity in

particles from wood smoke comparing traffic-related PM. In terms of the inflammatory potential, traffic-related PM has been found more potent than wood smoke in studies where exposure is longer than 12 hours (Kocbach et al., 2008b; Karlsson et al., 2006; Veronesi et al., 2002). On the contrary, another study by Kocbach et al. (2008a) with exposures shorter than 12 hours, results in similar inflammatory response for traffic-related and wood smoke PM. The inconsistency in these studies with different exposure time may indicate that the underlying mechanisms for the two exposures to induce inflammation may be different and thus have different patterns of effect with increasing exposure time. In a study on allergic effects, wood smoke seems to exhibit less capacity of allergic sensitization than diesel exhaust particles (Samuelsen et al., 2008). These discrepancies in different studies may be attributed to many factors, including the difference in the collected PM defined as "wood smoke" or "traffic-related PM", different measurements of indicators and outcomes, different toxicological behavior, and mechanisms of the particles from the two sources that may not be captured in any specific experimental design.

Studies on wood smoke described above have mostly focused on wood smoke from domestic heating instead of wildfire smoke. The characteristics and toxicity of PM from domestic wood smoke and wildfire smoke may be different for a variety of reasons. Firstly, the conditions of the fuel and the combustion environment are different for domestic heating and wildfire. Secondly, the chemical components of the PM can be transformed to a large extent during the transport of the wildfire smoke while most studies analyze exposure to domestic wood smoke freshly produced. Only a few toxicological studies have examined the toxicity of wildfire smoke PM specifically. Jalava et al. (2006) studied the inflammatory and cytotoxic effects of size-segregated PM from long-range transport of wildfire smoke in Finland. PM

from wildfire smoke showed lower activity in cytokine production compared with PM of corresponding sizes from typical ambient air pollution. However, it suggested that enhanced cytotoxic activities per inhaled cubic meter of air were associated with wildfire episodes because of the greatly increased PM of accumulation size range, which was related to high cytotoxixity. Wegesser et al. (2009) found that exposure to PM from wildfire in California induced about 10-fold more damage to the lung in mice than normal ambient aerosols from the same areas on an equal-dose basis, as measured by the evaluating several biomarkers of lung function damage.

1.3.2.2 Epidemiologic studies on the population effects of wildfire smoke.

Epidemiologic studies are critical for evaluating the health impacts of wildfire smoke because they investigate health responses in human populations. Naeher et al. (2007) reviewed epidemiologic studies on health effects from biomass burning in general. The work summarized that several studies had found associations between wildfire and respiratory tract illnesses, respiratory symptoms, and decreased lung function. Dennekamp & Abramson (2011) conducted a review on respiratory health effects from vegetation fires in Asia-Pacific region. They report that the association between respiratory morbidity and exposure to bushfire smoke was consistent with the associations found with urban air pollution. Henderson & Johnston (2012) reviewed eight studies with varied approaches to wildfire smoke exposure assessment and varied measures of respiratory outcomes and found consistent association between exposures and outcome. Table 1.2 provides a summary of selected studies that were published since 2006. These studies suggests that sufficient evidence has been found to associate wildfire smoke PM exposure with increased respiratory response symptoms, especially in people with pre-existing respiratory diseases such as COPD and asthma, consistent with

the three reviews mentioned previously. Evidence supporting the cardiovascular effects, which is very limited in the previous reviews, has been reported in some recent studies. The possibility and plausibility of the cardiovascular effects from wildfire smoke exposure is based on studies of changes in biomarkers related to cardiovascular diseases, such as the bone marrow response and systemic inflammation in forest firefighters as well as the general population, after exposure to wildfire smoke PM (Tan et al., 2000; Swiston et al., 2008). A recently published study reported that maternal exposure to wildfire events was associated with slightly lower infant birth weights, but also suggested that more investigation was needed in order to confirm this association as well as to assess alternative mechanistic pathways besides exposure to wildfire smoke (such as impact of mental stress resulting from the fire events) (Holstius et al., 2012).

Table 1.2 Summary of epidemiologic studies of health effects from wildfire smoke published since 2006.

Exposure assessment	Endpoints measured	Results	location	Reference
Aerosol optical depth by satellite to decide peat fire smoke density	Emergency Department visits	Significant increase in relative risk for asthma, chronic obstructive pulmonary disease, pneumonia and acute bronchitis, cardiopulmonary symptoms and heart failure were observed in smoke exposed counties.	North Carolina, US	(Rappold et al., 2011)
PM_{10} from nearest monitoring stations and a dispersion model; smoke coverage from remote sensing data	Physician visits; Hospital admission	Elevated PM_{10} from forest fire smoke is associated with increased respiratory physician visits and hospital admissions. Association with cardiovascular outcomes found to be largely null.	British Columbia, Canada	(Henderson et al., 2011)
Monitoring stations PM_{10}	Mortality; Hospital admission	A 10 mg/m^3 increase in forest fire PM_{10} was associated with a 1.24% (95% CI: 0.22–2.27%) increase in all respiratory hospital admissions.	Sydney, Australia	(Morgan et al., 2010)
Monitoring stations $PM_{2.5}$ to identify fire period	Emergency Department visits	No significant increase in emergency department admission rate of patients with cardiac and pulmonary morbidity after fire.	San Diego, US	(Schranz et al., 2010)
Monitoring stations PM_{10}, Airborne Particle Index for fine particles	Emergency Department visits; Hospital admission	A 9.1 mg/m^3 increase in PM_{10} was associated with a 1.8% (95% CI: 0.4–3.3%) increase in respiratory-related ED presentations in Melbourne. No association with hospital admission was found after adjustment for confounders.	Melbourne and Gippsland Region, Australia	(Tham et al., 2009)
Monitoring station PM_{10}	Physician visits	PM_{10} level found to be a significant predictor for health care seeking for respiratory illness, circulatory illness, coronary artery disease and headache.	Hoopa Valley Indian Reservation, CA, US	(Lee et al., 2009)

Table 1.3 Summary of epidemiologic studies of health effects from wildfire smoke published since 2006. ***(Continued)***

Exposure assessment	Endpoints measured	Results	location	Reference
Zip-code level $PM_{2.5}$ using spatial interpolation from measured $PM_{2.5}$, satellite smoke image and other factors	Hospital admission	Respiratory admissions strongly associated with $PM_{2.5}$ level during than before and after fires. Limited evidence of impact on cardiovascular admissions.	Southern California, US	(Delfino et al., 2009)
PM_{10} derived from visibility data by predictive model	Hospital admission	An increase of 10 $\mu g/m^3$ in same-day estimated ambient PM_{10} was associated with a 4.81% (95%CI: -1.04%, 11.01%) increase in total respiratory admissions. Negative association found for cardiovascular admissions for same day exposure while non-significant positive association found two or three days later.	Darwin, Australia	(Hanigan et al., 2008)
Monitoring station PM_{10}	Hospital admission	Positive relationship found between PM10 and admissions for all respiratory conditions (OR: 1.08, 95%CI: 0.98–1.18). No association between PM_{10} and cardiovascular admissions overall.	Darwin, Australia	(Johnston et al., 2007)
Monitoring stations PM_{10}, $PM_{2.5}$	Emergency Department visits	Increased PM concentration above the federal standard resulted in a significant increase in hospital emergency room visits for asthma, respiratory problems, eye irritation, and smoke inhalation.	San Diego, US	(Viswanathan et al., 2006)
Monitoring stations PM_{10}, $PM_{2.5}$ to identify fire period	Physician visits	Increased physician visits for respiratory diseases observed in one of the two communities impacted by smoke. No increase in cardiovascular and mental disease visits.	British Columbia, Canada	(Moore et al., 2006)

1.3.3 Wildfire smoke PM exposure assessment and prediction

1.3.3.1 Monitoring network

Wildfire smoke exposure assessment is vital to both epidemiologic researchers and public health practitioners. Conventional exposure assessment in epidemiologic studies relies largely on air quality monitoring networks. Table 1.2 summarized the exposure assessment methods used in some recent epidemiologic studies, and surface measurements were the most common method used. In terms of public health protection, tools such as the Air Quality Health Index (AQHI) in Canada and Air Quality Index (AQI) in the United States, monitor and forecast air quality also based on surface monitoring networks, and they have been commonly used to inform the public with advice on proper actions to protect their health during air pollution events, including wildfire smoke episodes.

Although most commonly used, exposure assessment or public health communication tools based on monitoring networks have two important limitations. First, they are not applicable to places where monitoring stations are not available, which tend to be the more sparsely populated areas where wildfires often burn. Second, PM measurements from monitors can be invalid during heavy smoke periods due to high PM mass loadings, or due to stations being incapacitated from direct fire damage (Wu et al., 2006). Efforts have been made to develop tools to supplement these limitations. For example, methods have been developed to estimate AQHI during wildfire events using visibility measurements, which can be done simply by observing visible landmarks at a wide range of distances with no special equipment and minimal training. Such estimates can be made in areas where typical air quality monitoring stations are not available (Taylor et al., 2012). Table 1.3 presents the $PM_{2.5}$ concentrations and AQHI that can be estimated by the corresponding visual range measurements.

Table 1.4 The tool estimating $PM_{2.5}$ concentrations and AQHI from visual range measurements (Taylor et al., 2012).

Visual Range (kilometres)	$PM_{2.5}$ (3-hr avg., μg/m^3)	AQHI
Greater than 35	0 to 15	1 to 3 - Low risk
8 to 35	15 to 65	4 to 6 - Moderate risk
3.5 to 8	65 to 150	7 to 10 - High risk
< 3.5	>150	11+ - Very high risk

1.3.3.2 Satellite remote sensing

Remote sensing can be defined as "the measurement of object properties on the earth's surface using data acquired from aircraft and satellites" (Schowengerdt, 2007, p.2). In other words, remote sensing is measuring the object of interest at a distance, without physical contact. Satellite remote sensing has been applied for atmospheric aerosol observation over the past 30 years (Lee et al., 2009). The theory of aerosol observation by remote sensing is to record radiation emitted either by the sun (passive sensor instruments) or by the sensor itself (active sensor instruments) that is reflected back to the sensor. After decomposing the reflectance signals emanating from atmospheric gases, aerosols, and the surface, information about the aerosol thickness and other properties can be retrieved (Lee et al., 2009). Wildfire smoke, consisting of high concentrations of aerosols, can also be observed by remote sensing tools. Referring back to Table 1.2, there are some examples where exposure estimates incorporated or were totally based on remote sensing techniques.

The Moderate Resolution Imaging Spectroradiometer (MODIS) is an instrument carried by the Terra and Aqua satellites. The instruments can acquire data in 36 spectral bands, measuring large-scale processes in the oceans, on land, and in the lower atmosphere (NASA,

2012). Some of its products have been widely used for wildfire smoke observations, including the MODIS true color images and the Aerosol Optical Depth (AOD). Figure 1.2 Shows the MODIS true color image and AOD on 16 August, 2001, capturing widely dispersed wildfire smoke in the Lower Fraser Valley of BC.

Another widely used smoke identification and assessment tool based on remote sensing data is the Hazard Mapping System (HMS) Fire and Smoke Product developed and maintained by the National Oceanic and Atmospheric Administration (NOAA) in the United States (US). HMS is an interactive processing system in which trained analysts manually integrate data from various automated fire detection algorithms with images from different satellites and remote sensing instruments. Images are obtained from a total of seven satellites operated by NOAA and the US National Aeronautics and Space Administration (NASA) to provide continuous monitoring (Table 1.4). By incorporating the data from different satellites and instruments, their individual limitations in spectral, temporal, or spatial resolution can be largely overcome. Separate automated fire detection algorithms are applied to images obtained from different instruments, while all of these algorithms are based on a certain temperature threshold reached at a certain spectral channel within the infrared radiation bandwidth of the sensor. In other words, if the temperature detected by a spectral channel at a certain wavelength is significantly increased, the associated pixel will be identified as hotspot, indicating a potential fire event. Table 1.5 provides a summary of the algorithms used by different instruments. A standardized procedure is followed by trained NOAA analysts to delete false detections resulting from heat sources other than fires, and to add hotspots missed by automated detections. After this process is complete, visible imagery is used by analysts to manually derive the outlines of smoke plumes. The final output is a display of the fire loca-

tions and the outline of the smoke plumes over North America. A semi-quantitative estimate of the smoke concentrations (in several concentration categories) is made for each smoke plume based on the AOD data from the GOES Aerosol and Smoke Product (NOAA, 2011; Ruminsk et al., 2006).

Remote sensing data can provide exposure estimates at a much finer spatial resolution than monitoring networks, and are available for places not covered by monitoring networks. On the other hand, there are some limitations for remote sensing data. First, they measures the total column of air pollutants in the atmosphere rather than the ground level concentrations of most concern to public health. At present there is no validated algorithm to convert columnar measurements to the ground level fraction. The development of such an algorithm is complex and location specific, requiring intensive research efforts. Second, clouds and some specific land surfaces can affect the performance of remote sensing instruments.

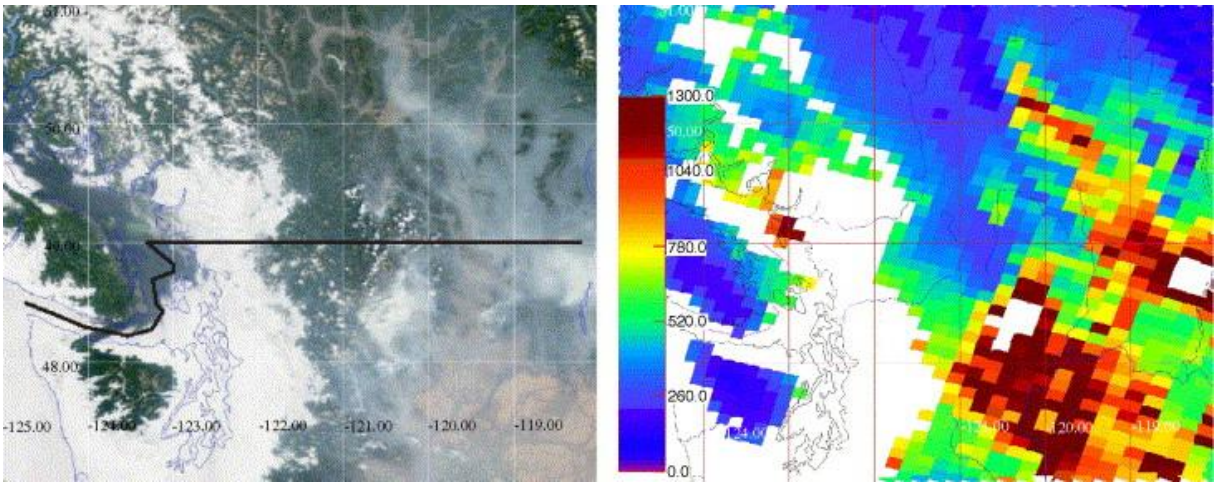

Figure 1.2 MODIS true color image (left) and aerosol optical depth (right) on 16 August, 2001, showing a widely dispersed smoke plume east of 121 ℃W longitude in Lower Fraser Valley of British Columbia (Leithead et al., 2006).

Table 1.5 Remote sensing data sources for Hazard Mapping System (HMS).

Data collected	Satellite	Instrument	Features
Geostationary data	GOES-10 GOES-12	3.9 μm band and visible band sensors	High temporal resolution Nominal spatial resolution
Polar orbiting data	NASA-Terra NASA-Aqua	Moderate Resolution Imaging Spectro-radiometer (MODIS)	High spatial resolution Low temporal resolution
	NOAA-15 NOAA-17 NOAA-18	Advanced Very High Resolution Radiometer (AVHRR)	

Table 1.6 Fire detection algorithms for remote sensing instruments used in HMS.

Instrument	Algorithm	Reference
GOES	WildFire-Automated Biomass Burning Algorithm: If the observed brightness temperature for a pixel shows at least 4 Kelvin (K) and 1K increase over the background temperature for the 3.9μm and 11.2μm spectral channels, respectively, it is identified as hot spot.	(Prins & Menzel, 1992)
MODIS	Examine each pixel by exploiting the strong emission of infrared radiation at the 4μm and 11μm channel (i.e. the detected temperature T4 and T11). If T4>310 K, T4 -T11>10 K, a potential fire spot will be identified. More information from different channels will be included to assign classes of missing data, cloud, water, non-fire, fire or unknown to each pixel.	(Giglio et al., 2003)
AVHRR	Fire Identification, Mapping and Monitoring Algorithm: Use a threshold value of 320K for brightness temperature at the 3.7μm channel images to identify potential fire pixels and use multi-channel information to remove false detects.	(Li et al., 2000)

1.3.3.3 Forecasting models

Both data from monitoring stations and remote sensing platforms can only provide retrospective or near-real-time observations of air quality during wildfire events. From the perspective of public health protection, a tool that can effectively predict wildfire smoke in advance would be even more valuable. Forecasts have been implemented to communicate with the public about many other potential health hazards, such as ultraviolet radiation, temperature, air quality, and pollen counts. By having tools to predict the hazard in advance, more timely actions can be taken to inform the public and to provide information about mitigating the adverse impacts before the exposure actually occurs. Given that wildfire smoke in North America usually is a short-term exposure that can reach extremely high concentrations, the timing of these actions is especially important. This is one of the motivations for developing a wildfire smoke forecasting system.

In Europe, there is an operational wildfire-induced smoke forecasting framework (http://silam.fmi.fi/, Sofiev et al., 2009) based on the combination of two systems: the Fire Assimilation System (FAS), which evaluates the emission fluxes of primary PM from wildfires, and a chemical transport model called the System for Integrated Modeling of Atmospheric Composition (SILAM). The FAS consists of two parallel branches based on the Temperature Anomaly (TA) and Fire Radiative Power (FRP) measurements from the MODIS Collection 4 and 5 Active Fire Products. The fire detection algorithm of MODIS has been mentioned previously in Table 1.5, and Table 1.6 describes the algorithms used for these two branches to convert fire information to $PM_{2.5}$ emissions. Estimations of emissions will then be input to the SILAM with meteorological information to compute the dispersion of fire

smoke PM at a 25 km spatial resolution with 10 vertical layers up to 8 km of the altitude, over the whole of Europe (Sofiev et al., 2009).

In the US, NOAA started to produce daily operational smoke particulate ($PM_{2.5}$) forecast in 2007, using the NOAA Smoke Forecasting System (SFS) (Rolph et al., 2009). Table 1.7 provides brief descriptions of the models and databases used in this system. Fire hotspots that may lead to continuous smoke emissions are identified by HMS, described in Section 1.3.3.2. Predictions of $PM_{2.5}$ emissions are made based on fire location and size, using the emissions estimation module of the BlueSky smoke modeling framework. BlueSky is a fire and smoke prediction tool originally developed to assist with wildfire containment and prescribed burn decisions by considering information about fuel conditions and consumption (Table 1.7). Emissions estimates and meteorological forecasts from the two models (Table 1.7) are both input for the Hybrid Single-Particle Lagrangian Integrated Trajectory (HYSPLIT) dispersion model, which produces smoke forecasts over North and Central America once daily. The output is a 15 km resolution grid of hourly (up to 60 hours in advance) averaged air concentrations of $PM_{2.5}$ in the lowest 100 m layer, comparable with surface air quality measurements (Rolph et al., 2009).

Table 1.7 Algorithms of converting fire information to $PM_{2.5}$ emissions in the Fire Assimilation System.

Branch	Input fire data	Conversion
TA	Pixel brightness temperature	Multiplied with an empirical coefficient obtained from the calibration between pixel brightness temperatures and surface observations of $PM_{2.5}$ downwind of the fire in a fire episode in 2006.
FRP	FRP data *	Multiplied with empirical coefficients for three different land uses obtained from the calibration between FRP and total column PM derived from the aerosol optical depth (AOD) observed by MODIS according to a study by Ichoku and Kaufman (2005). Then relate the total PM to $PM_{2.5}$ according to factors reported by Andreae and Merlet (2001).

*FRP is calculated as a function of the brightness temperature difference between the fire pixel and the neighboring pixels.

Table 1.8 Descriptions of models/databases involved in the NOAA Smoke Forecasting System.

Model/Database (Reference)	Description
CONSUME (FERA, 2011)	Import fuel characteristics data directly from the Fuel Characteristic Classification System (FCCS), and output fuel consumption and emissions by combustion phase. It can be used for most forest, shrub and grasslands in North America.
NFDRS (National Wildfire Coordinating Group, 2002)	Provide ratings describing conditions that reflect the potential for a fire to ignite and spread, taking into account factors including the ignition temperatures of woody material, rates of combustion, the moisture of extinction of various types of plant material, the chemical properties of woody debris, and heat energy potential.
NAMWRF (NCEP, 2012a)	A regional, non-hydrostatic weather forecast system for North America producing hourly forecasts in horizontal grid resolution of 12km out to 84 hours.
GFS (NCEP, 2012b)	A global, spectral, hydrostatic weather forecast system producing forecasts in horizontal grid resolution of 80km out to 384 hours.
HYSPLIT (ARL, 2011; Rolph et al., 2009)	A dispersion model calculating advection and diffusion within a Lagrangian framework following the transport, while calculating concentrations on a fixed grid in Eulerian approach. Transport and dispersion calculation base on assuming: • Puff dispersion: released puffs expand until they exceed the size of the meteorological grid cell (either horizontally or vertically) and then split into several new puffs, each with its share of the pollutant mass. • Particle dispersion: turbulent dispersal of an initial fixed number of particles. • Puff dispersion in horizontal and particle dispersion in vertical direction.

1.3.4 BlueSky Western Canada Smoke Forecasting System

BlueSky is a modeling framework that was originally developed and maintained by the US Forest Service AirFire Team for fire and smoke prediction. It is a tool that modularly links different datasets and models. Basic modules within the framework include fuel loading, total consumption, time rate of consumption, emissions, plume rise, and dispersion. New modules can be added by users to suit their own needs. The determination of the specific models and databases for each module depends on the region where the prediction is made, the specific purpose, and the output requirements. This framework has been applied in a

number of regional and national smoke and air quality prediction systems in North America (AirFire, 2010).

The need for an operational smoke forecasting system in Canada was identified in 2007. A pilot project to apply the BlueSky framework to BC and Alberta (BlueSky Western Canada) was started in 2008. The conceptual outline of the system is illustrated in Figure 1.3. The framework of this system is very similar to the NOAA SFS, with different inputs, such as a different meteorological model and a different fire information processing system.

Fire information is obtained from the Canadian Wildland Fire Information System maintained by Natural Resources Canada. The Fire Monitoring, Mapping and Modelling system produces information about fire location and size derived from hotspots detected from satellite sensors including AVHRR, MODIS, Satellite Pour l'Observation de la Terre Vegetation, Landsat's Thematic Mapper, and some thermal infrared scanners flown on board aircraft for fire hotspots and fire intensity mapping over individual fires or small regions. The Canadian Forest Fire Behavior Prediction system produces output including rate of fire spread, total fuel consumption, and head fire intensity based on the input of fuel type maps developed by satellite image-based land cover classification and the National Forest Inventory. It also includes weather, topography, foliar moisture, and other variables. (Sakiyama, 2011; Natural Resources Canada, 2011) These data are input for the Fire Emission Production Simulator to compute the plume rise and emissions of $PM_{2.5}$.

Meteorological information and prediction are produced by the Fifth-Generation PSU/NCAR mesoscale model, known as MM5, run at the University of British Columbia (UBC). MM5 is “a limited-area, nonhydrostatic, terrain-following sigma-coordinate model designed to simulate or predict mesoscale and regional-scale atmospheric circulation”

(UCAR, 2008), and it can be relocated to support predictions globally by incorporating local geographical characteristics and meteorological observations. The MM5 implementation at UBC provides 4 km grid resolution hourly weather forecast two days in advance for BC and Alberta. After the enhancement in 2011, forecasts in 12 km grid resolution for southern portions of the Yukon, Northwest Territories and Nunavut and the northern US border States (Washington, Idaho, Montana, North Dakota, and Minnesota) are also available to support the domain expansion. Data needed from MM5 for HYSPLIT input include wind direction and wind speed (Sakiyama, 2011). Emissions and meteorology information are then input to the HYSPLIT model (see description in Table1.7) to calculate dispersion and, ultimately, ground level $PM_{2.5}$ concentrations. The animation and Google Earth files of these hourly $PM_{2.5}$ concentration forecasts have been publicly available online[1] since 2010.

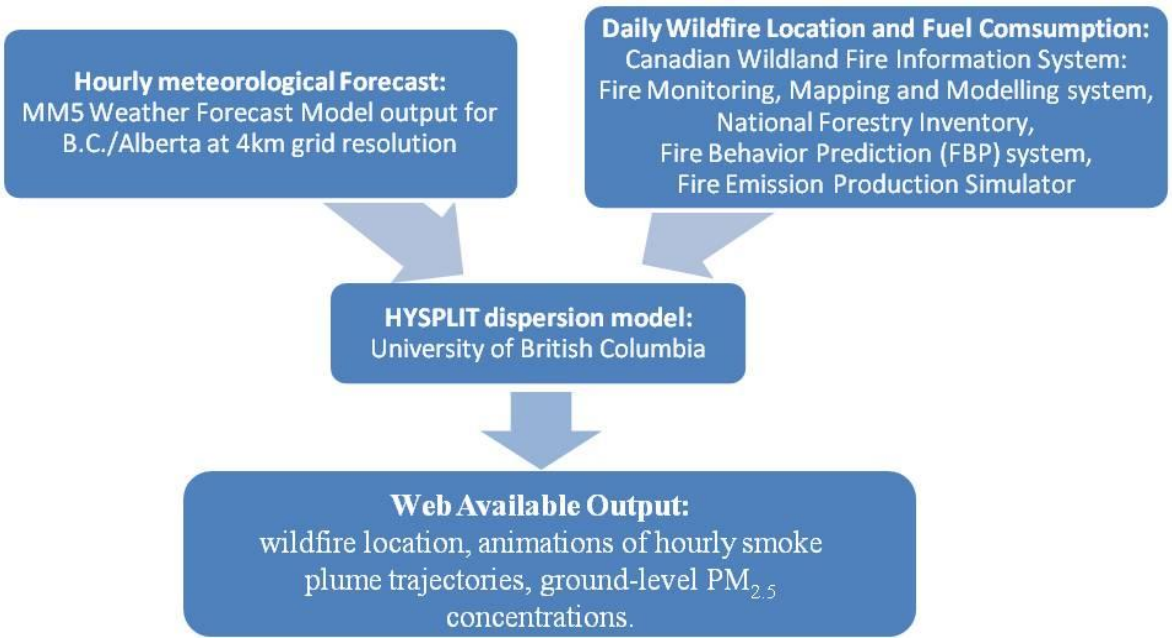

Figure 1.3 Conceptual outline of the BlueSky Western Canada smoke forecasting system (Sakiyama, 2011)

[1] Smoke Forecasts for Western Canada: http://www.bcairquality.ca/bluesky/

After its operation in the 2010 fire season, several improvements were made to Western Canada Bluesky before the 2011 fire season. Firstly, the output of the enhanced system was extended from 45N to 65N and from 85W to 145W in a latitude-longitude grid with 0.1 degree spacing. Secondly, smoke from wildfires in the US border States was included in the forecasts (Sakiyama, 2011). Thirdly, persistent smoke, which lasted through the forecast period, was included.

1.3.5 Previous evaluation of wildfire smoke forecast system

A model needs to be evaluated with other comparable measurements to assess its performance. Different statistical methods to evaluate model performance, both spatially and temporally, were described by Mosca et al. (1998). In this thesis, two major aspects were tested: the correlation and difference between the modeled and reference $PM_{2.5}$ concentrations (e.g. BlueSky $PM_{2.5}$ estimates vs. monitoring station $PM_{2.5}$ measurements), and the extent of spatial overlap between modeled and reference plume trajectories (e.g. BlueSky plumes vs. HMS plumes). An indicator called the figure of merit in space (FMS) was used to evaluate the extent of overlap, , which is defined as "the percentage of overlap between the measured and predicted areas":

$$\mathrm{FMS} = \frac{\mathrm{A_{OB}} \cap \mathrm{A_{PR}}}{\mathrm{A_{OB}} \cup \mathrm{A_{PR}}} \times 100\%$$

Where A_{PR} = area of the prediction, and A_{OB} = area of the observation, $A_{\mathrm{OB}} \cap A_{\mathrm{PR}}$ is the intersection of the plume areas of observation and prediction, and $A_{\mathrm{OB}} \cup A_{\mathrm{PR}}$ is the union of the two plume areas.

Sofiev et al. (2009) evaluated the European fire assimilation system by comparing its predictions during two fire episodes with total PM mass in atmospheric columns derived

from MODIS observations and in-situ observations of PM_{10} at monitoring stations. Individual mean values and correlation coefficients between observations and predictions were computed as indicators of agreement. Predicted PM mass differed by approximately 30% from the observations, and the correlation coefficients were 0.3 and 0.5 for the TA and FRP branches, respectively.

The performance of the NOAA SFS in the 2007 fire season was evaluated by Rolph et al. (2009). The FMS described by Mosca et al. (1998) and another indicator called measure of effectiveness (MOE) were used as indicators of the spatial agreement between SFS predictions, with the HMS plumes as the reference. MOE is a two-dimensional measure introduced by Warner et al. (2004), described as:

$$\mathrm{MOE} = (x, y) = \left(\frac{A_{OV}}{A_{OB}}, \frac{A_{OV}}{A_{PR}}\right) = \left(\frac{A_{OB} - A_{FN}}{A_{OB}}, \frac{A_{OB} - A_{Fp}}{A_{PR}}\right) = \left(1 - \frac{A_{FN}}{A_{OB}}, 1 - \frac{A_{FP}}{A_{PR}}\right)$$

where A_{FN} = area of false negative, A_{FP} = area of false positive, A_{OV} = area of overlap, A_{PR} = area of the prediction, and A_{OB} = area of the observation. FMS scores during three fire events between the NOAA SFS 24-hour predicted and HMS observed plumes ranged from 0.02 to 0.40

Larkin et al. (2009) performed a case study evaluation of the BlueSky smoke modeling framework applied in the United States at two locations. The focus of the study was inter-model evaluation, primarily investigating the impact of model choices within the BlueSky framework. The forecasting output was compared visually with plumes observed by satellites (HMS and MODIS) and predicted values were compared with data from monitors using box-plots. The results suggest that the output is sensitive to choices regarding different fuel loading, consumption models, and assumptions about the fire behavior (number of fire plumes derived from the released heat). Agreement between plume shapes was generally good, and

estimated concentrations generally underpredicted the surface measurements, but no statistical results were reported. The highest FMS score for individual events was found to approach 60% and the average scores were around 10%.

An unpublished report by Klikach (2011) evaluated the performance of the BlueSky Western Canada System in Alberta. It examined the magnitude, timing, and shape of the monitoring observations versus the predictions from BlueSky, by simple time-series plotting and comparison of the descriptive statistics. It concluded that BlueSky tended to underpredict $PM_{2.5}$ concentrations, and that estimates dropped off quickly while the smoke continued to linger at the monitoring sites. In addition, the model tended to predict the peak of a fire event too early. While this study provided many qualitative insights on the model performance, the utility of its conclusions is limited by its lack of sophisticated statistical analysis.

Overall, there has been few systematic evaluations of BlueSky performanceto date, and none in BC. This thesis research fills the knowledge gap, and provides valuable information for the ongoing development of the system. More importantly, this study is the first to report the association between wildfire smoke predictions and population health outcome measures. To support the use of predictions from a forecasting model for advising public health actions, evidence on this association is needed.

There are two main components in this thesis study: (1) evaluation of the BlueSky prediction model and (2) assessment of the association between BlueSky predictions and health outcomes. Chapters 2 and 3 will describe the methods and results for these two components, respectively.

2. BlueSky prediction model evaluation

This chapter describes the first part of the thesis study, which is to evaluate the performance of the Western Canada BlueSky System in BC during the 2010 fire season by (1) comparing the BlueSky $PM_{2.5}$ predictions with ground-level monitoring stations measurements, and (2) comparing the shape and size of BlueSky plumes with those recorded by the Hazard Mapping System (HMS, described in Section1.3.3.2).

2.1 Methods

This section illustrates the methods used in the process of data collection and preparation, as well as the statistical analyses applied for model evaluation. Section 2.1.1 describes the process of data collection and preparation. In this process, BlueSky predictions, HMS smoke plume images, and monitoring $PM_{2.5}$ measurements were retrieved. They were converted to proper formats ready for display and manipulation. Hourly predictions and measurements were used to calculate daily averages. Section 2.1.2 introduces the statistics used for comparing locations, sizes, and shapes of smoke plumes predicted by BlueSky and observed by HMS images. It also introduces the statistics for the three types of analyses used to compare the agreement between BlueSky $PM_{2.5}$ predictions and measured concentrations.

2.1.1 Data collection and preparation

2.1.1.1 BlueSky predictions

The BlueSky data were retrieved in June, 2011 from the server in the Department of Earth and Ocean Science, University of British Columbia, where the BlueSky model was run. The data obtained were "rerun" predictions for July 24 to August 29th, 2010, a time frame covering the major wildfire events in 2010 season (see Section 1.1.3). By "rerun" predictions, it is meant that the 2010 fire smoke emissions and meteorological data were used as input to compute the predictions using the newly improved BlueSky system in 2011. As mentioned in Section 1.3.4, after the official launch in 2010, the BlueSky system was improved for the 2011 season. Evaluating the new system was more appropriate for our goal. As shown in Figure 2.1, predictions were run once daily for the next 60 hours, beginning with 00:00 Co-ordinated Universal Time (UTC) time.

Hourly predictions were converted to formats that could be read and analysed, and then the daily averages were calculated. When originally retrieved from the server, the output of predictions from each run were contained in a single NetCDF file, a format that could not be read and manipulated using conventional tools. Thus, the data were converted to 60 ASCII files of hourly predictions and two ASCII files of daily average of these hourly predictions by running scripts in Python 2.7 and R (version 2.13.0) (see Figure 2.2). These scripts are attached in Appendix A. The daily average was calculated from hourly files from midnight to midnight in Pacific Daylight Time (PDT), as the analysis was restricted in British Columbia. The first daily average was calculated with the first 24 hours of a complete day in PDT time, and the second daily average was calculated with the 24 hours in next complete day. For example (see Figure 2.1), from the predictions made at 17:00 PDT on July 23rd, we would have

a 24-hour prediction for July 24th and a 48-hour prediction for July 25th.

The ASCII files of daily averages were imported in ArcMap 10.0 (ESRI, Redlands, California) and converted to raster files using the "ASCII to raster" conversion tool. The outline of the raster pixels with values larger than zero was defined as BlueSky Plume, which could then be compared with the HMS Plume defined in Section 2.1.1.2.

In order to compare the BlueSky $PM_{2.5}$ estimates with the monitoring measurements, values from the raster file at the selected monitoring locations (see Section 2.1.1.3) were extracted using the spatial analysis tool "Extract values to points". This process is presented in Figure 2.3.

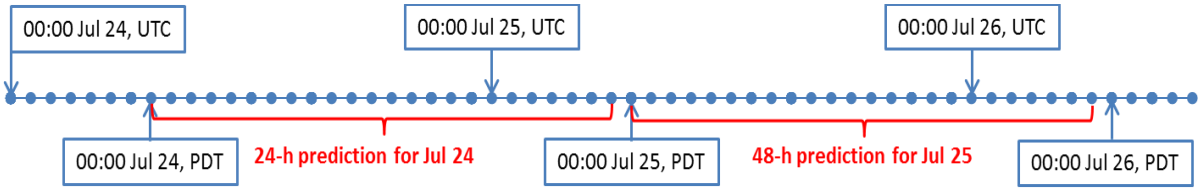

Figure 2.1 Example of the two daily averages computed from predictions made on July 24th. Prediction made on each day includes 60 hourly predictions (the blue dots), beginning at 0:00 UTC time

.

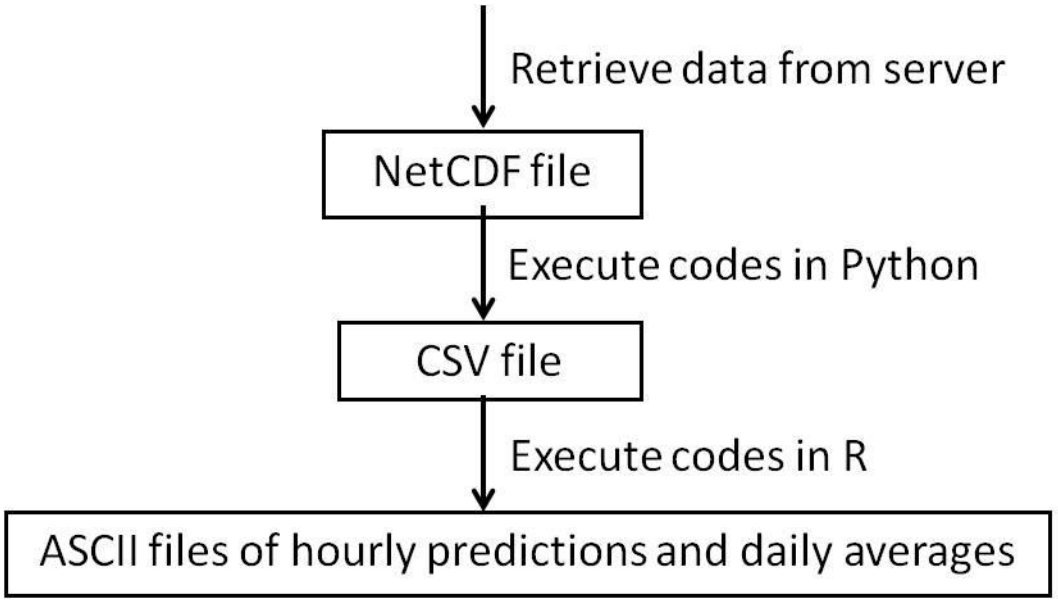

Figure 2.2 Diagram of data format conversion process.

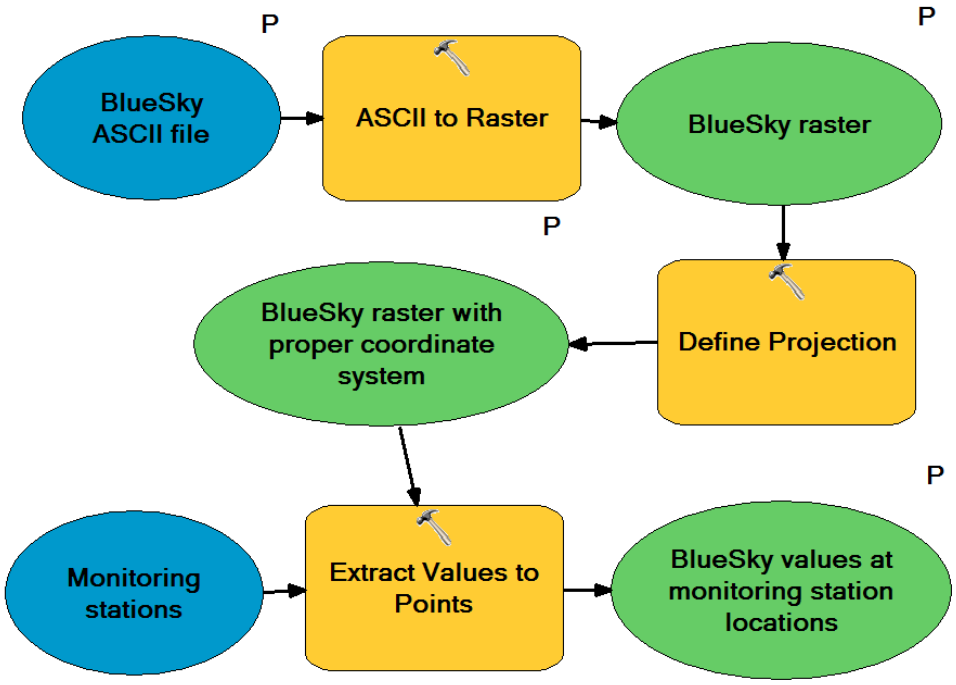

Figure 2.3 Process diagram of extraction of BlueSky values for monitoring locations in ArcGIS. Circles in blue indicate the input files. Squares in yellow indicate the ArcGIS tools used in the process. Circles in green indicate the outputs of each step.

2.1.1.2 Hazard Mapping System (HMS) Images

The shape and size of smoke plumes predicted by BlueSky were evaluated using HMS smoke plumes based on multiple satellite images. The daily images of smoke plumes from HMS were retrieved from a public ftp site maintained by NOAA. The data retrieved were in shapefile format, which could be imported directly into AcrMap for analysis. Each of the HMS image files included different layers of smoke plumes drawn during different times of the day, and a rough estimate of the smoke density assigned to each smoke plume layer by the NOAA analysts. In order to compare the plume extent with BlueSky plume, all of the HMS plume layers from a single day were dissolved into one combined plume, regardless of the density estimates. This was done in ArcMap using the "Dissolve" tool (see Figure 2.4). The semi-quantitative estimates of smoke density for the HMS plumes were not used in our

analysis. Every HMS smoke plume was in fact the "footprint" of the smoke detected by one or several instruments during multiple time periods in a day. In other words, smoke could be travelling anywhere within the smoke plume outline during the period and the exact time during which the smoke of a certain density actually covered a specific region was not recorded. In addition, these observation time periods were varied between different smoke plumes recorded on a same day. These characteristics of the HMS plume data made it difficult to calculate a reasonable hourly or daily average of the smoke densities comparable with the BlueSky smoke plumes.

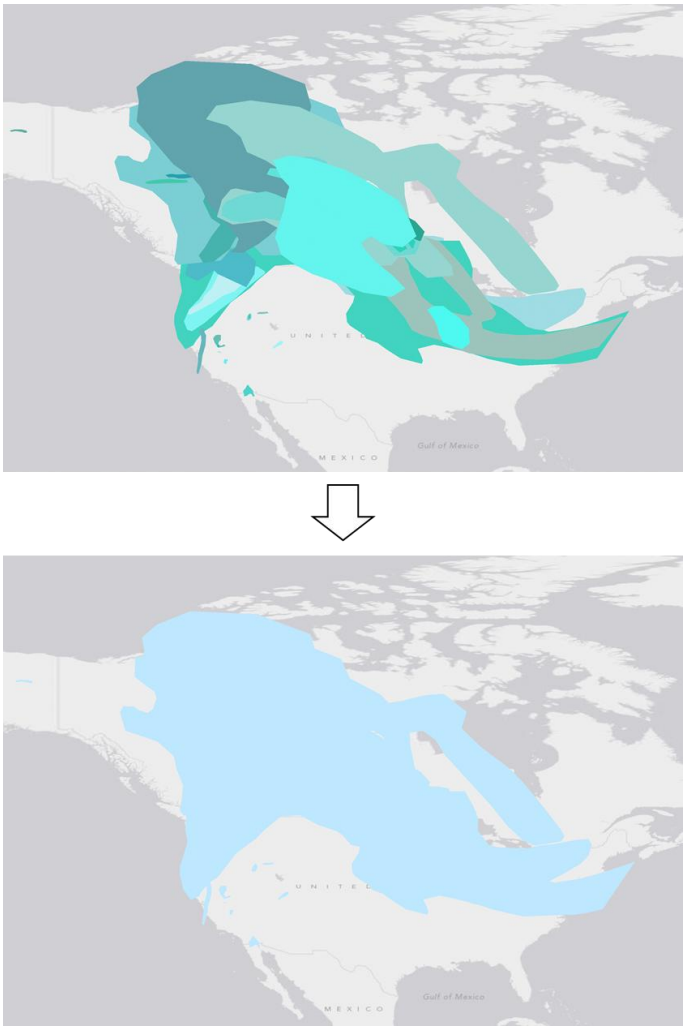

Figure 2.4 Diagram of dissolving multiple HMS smoke plumes in a day into one.

2.1.1.3 Monitoring Measurements

The accuracy of BlueSky $PM_{2.5}$ predictions was evaluated using ground-level monitoring station measurement. Hourly $PM_{2.5}$ measurements from a total of 55 ground-level monitoring stations in BC were retrieved from BC Ministry of Environment and Metro Vancouver. Locations of these monitoring stations in latitude and longitude were retrieved from the BC air data archive website maintained by the BC Ministry of Environment. As some regions had multiple monitors, 36 out of the 55 monitors were selected (see Figure 2.5). The selection was based on two criteria. First, only one monitor was selected for each place name (for example, there were four stations with a name beginning with "Prince George" and only one of them would be selected). The choice of specific monitor was based on the completeness of the data, meaning the one with more complete data during the study period would be chosen. Second, for a small geographical region with densely distributed monitors, such as the Lower Mainland, monitors with more complete data and more sensitive to forest fire smoke were selected. The sensitivity of the monitors to forest fire smoke was assessed using the study results by Keane (2012). This study compared $PM_{2.5}$ concentrations observed by monitors in Lower Mainland on days with and without forest fire smoke. Monitors with larger difference in $PM_{2.5}$ values on smoke and non-smoke days were considered to be more sensitive to fire smoke.

Daily averages were computed from the hourly records from midnight to midnight, PDT. The daily averages were set to missing if 6 hours or more of the hourly data in total, or 3 hours or more of the hourly data consecutively were missing on that day. Records of filter pressure (FP), a measure of the filter's loading, for the $PM_{2.5}$ measurement in corresponding monitoring stations were also retrieved from the BC Ministry of Environment website. When

FP was larger than 60%, the filter could be considered overloaded and the $PM_{2.5}$ measurement during these periods might not be reliable. As a result, data measured with FP larger than 60% were also considered missing. The FP data were not available for some of the monitoring stations selected (see Figure 2.5), but this was considered unlikely to affect the results because stations without FP records were in areas with limited wildfire smoke impact in 2010.

$PM_{2.5}$ concentrations were measured by either a tapered element oscillating microbalance (TEOM) or a Beta-Attenuation Mass (BAM) monitor. The instrument used in different monitoring stations is shown in Figure 2.5.

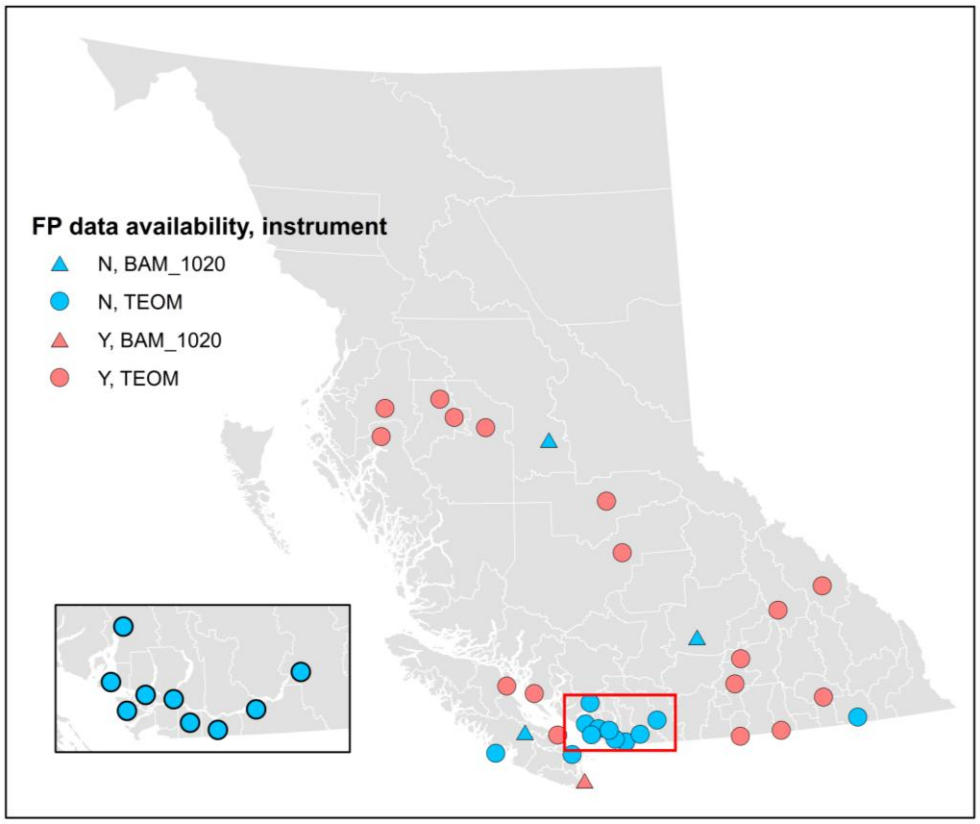

Figure 2.5 Monitoring stations selected to include in the evaluation and instrument used for PM measurement.

Circles and triangles indicate the use of BAM-1020 and TEOM, respectively. Labels in blue are stations without FP records (N) and those in red indicate stations with FP record available (Y).

2.1.2 Statistical Analyses

2.1.2.1 Comparison between BlueSky and HMS

The sizes and locations of smoke plumes were compared between BlueSky and HMS. BlueSky plumes were defined as the polygons of pixels with values larger than zero in the BlueSky prediction raster file. This approach was analogous to the approach of dissolving all HMS plumes into one plume, regardless of their density classifications.

As the scope of the study was set to be within BC, both the BlueSky and HMS plumes were first intersected with the BC boundary. Then the two plumes were overlaid in ArcMap, and the areas of the BlueSky plume ($A_{BlueSky}$), HMS plume (A_{HMS}), the intersection of the two ($A_{BlueSky} \cap A_{HMS}$) and the union of the two ($A_{BlueSky} \cup A_{HMS}$) were calculated for each day (Figure 2.6).

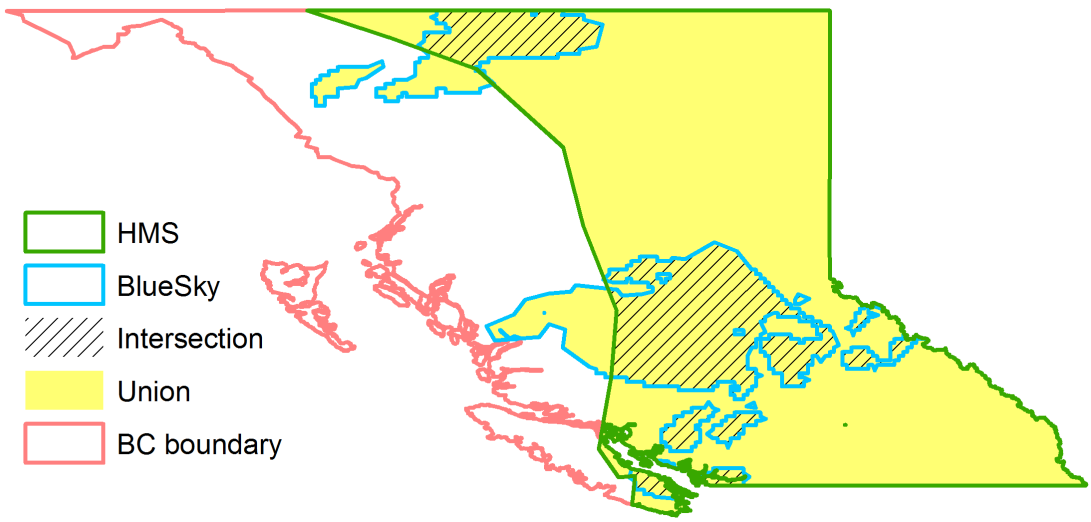

Figure 2.6 Illustration of plume overlaying in ArcGIS to calculate area of BlueSky and HMS plumes as well as their intersection and union.

To quantitatively assess the extent of agreement, a spatial statistic called the figure of merit in space (FMS) was applied (Equation 2.1). The FMS ranges from 0 to 1, with a higher FMS indicating better agreement between the HMS and BlueSky smoke plumes. Daily FMS values were plotted in time-series to show the spatial agreement between the two plumes at different time points.

$$FMS = \frac{A_{HMS} \cap A_{BlueSky}}{A_{HMS} \cup A_{BlueSky}} \times 100\% \qquad \text{Equation 2.1}$$

2.1.2.2 Comparison between BlueSky and monitoring measurements

The daily averages of BlueSky predicted $PM_{2.5}$ concentrations were compared with the monitoring station measured $PM_{2.5}$ concentrations by computing model evaluation statistics in three different analyses: global, temporal, and spatial. Together, these analyses showed the overall, temporal and spatial agreement between $PM_{2.5}$ predictions and measurements, respectively.

A total of four model evaluation statistics, including Pearson's correlation coefficient (r), index of agreement (IOA), normalized root mean square error (NRMSE), and fractional bias (FB) were calculated between values predicted by BlueSky and measured by monitoring stations. The formulas for these statistics are presented in Table 2.1.

In the **global analysis**, all predicted and observed values at any time and location were included in the calculation. The overall agreement and tendency to underpredict or overpredict was examined. Bland-Altman plots (Altman & Bland, 1983), which indicate the difference between prediction and measurement against the average of prediction and measurement, were also used in this analysis to visualize the overall agreement.

In the **spatial analysis**, BlueSky predicted and monitoring station observed values were compared at a fixed time for all locations. This analysis was used to examine whether locations with high/low observed concentrations had high/low predictions at a specific time.

In the **temporal analysis**, a whole time series of BlueSky predicted and monitoring station observed values was compared for a fixed location. This analysis was used to examine whether high/low predictions were made at a specific location when high/low concentrations were observed.

Table 2.1 Model evaluation statistics.

Statistics	Acronym	Formula*	Ideal value (range)
Correlation coefficient	r	$r = \frac{\frac{1}{N}\sum_{i=1}^{N}(O_i - \overline{O})(P_i - \overline{P})}{\sigma_P \sigma_O}$	1 [-1,1]
Index of agreement	IOA	$IOA = 1 - \frac{\sum_{i=1}^{N}(P_i - O_i)^2}{\sum_{i=1}^{N}(\lvert P_i - \overline{P}\rvert + \lvert O_i - \overline{O}\rvert)^2}$	1 [0,1]
Normalized root mean squared error	NRMSE	$NRMSE = \frac{\sqrt{\frac{1}{N}\sum_{i=1}^{N}(P_i - O_i)^2}}{O_{\max} - O_{\min}}$	0 [0,+∞]
Fractional Bias	FB	$FB = \frac{(\overline{P} - \overline{O})}{0.5(\overline{P} + \overline{O})}$	0 [-2,2]

* O_i = the ith observation from monitor, P_i = the ith prediction from BlueSky, $\overline{O}$ = the mean of observations, $\overline{P}$ = the mean of predictions, O_{max} = the maximum value of observations, O_{min} = the minimum value of observations, σ_O = standard deviation of observations, σ_P = standard deviation of predictions.

2.2 Results

2.2.1 Plume comparison between BlueSky and HMS

Figure 2.7 presents the daily smoke plume areas observed by HMS and predicted by BlueSky during the whole study period. The two peaks in smoke plume area clearly corresponded with the two major fire events. HMS generally produced larger smoke plumes than BlueSky during major fire events. This is also the conclusion from Table 2.2, which summarizes the smoke plume sizes in terms of absolute area and the percentage of BC covered. BlueSky 24-hour predictions produced slightly larger plumes than the 48-hour predictions, especially at the beginning of the fire events.

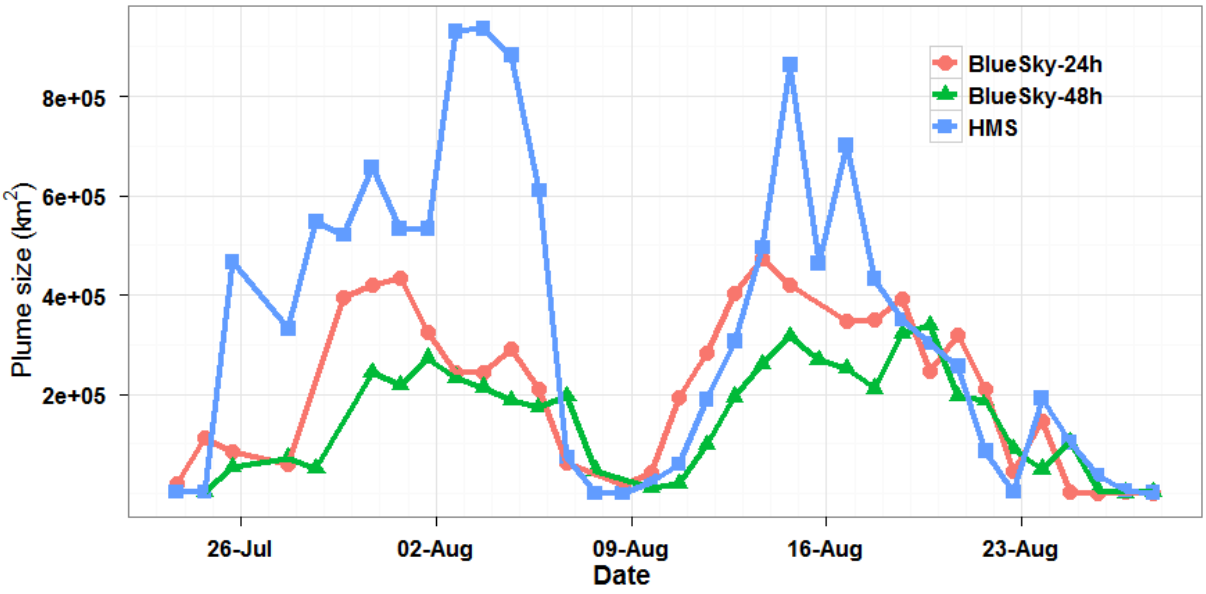

Figure 2.7 Smoke plume areas observed by HMS and predicted by BlueSky daily during the study period.

Figure 2.8 shows the daily FMS scores calculated from BlueSky and HMS. Higher FMS indicates better agreement in space between the observed and predicted smoke plumes. The mean FMS score for the 24-hour predictions was 0.18, with a range between 0 to 0.59. The mean FMS score for the 48-hour predictions was 0.21, with a range between 0 to 0.52. As indicated in the

figure, high FMS scores were observed during the major fire event periods. FMS scores for the 24-hour predictions were generally higher than the 48-hour predictions, especially at the beginning of the major fire events.

Table 2.2 Summary of smoke plume areas observed by HMS and predicted by BlueSky.

	Mean (km^2) (% of BC area)	Minimum (km^2) (% of BC area)	Maximum (km^2) (% of BC area)
HMS	334,500 (35.22%)	580 (0.06%)	936,400 (98.59%)
BlueSky-24h	212,500 (22.37%)	111 (0.01%)	474,400 (49.94%)
BlueSky-48h	153,200 (16.13%)	2,137 (0.23%)	338,500 (35.64%)

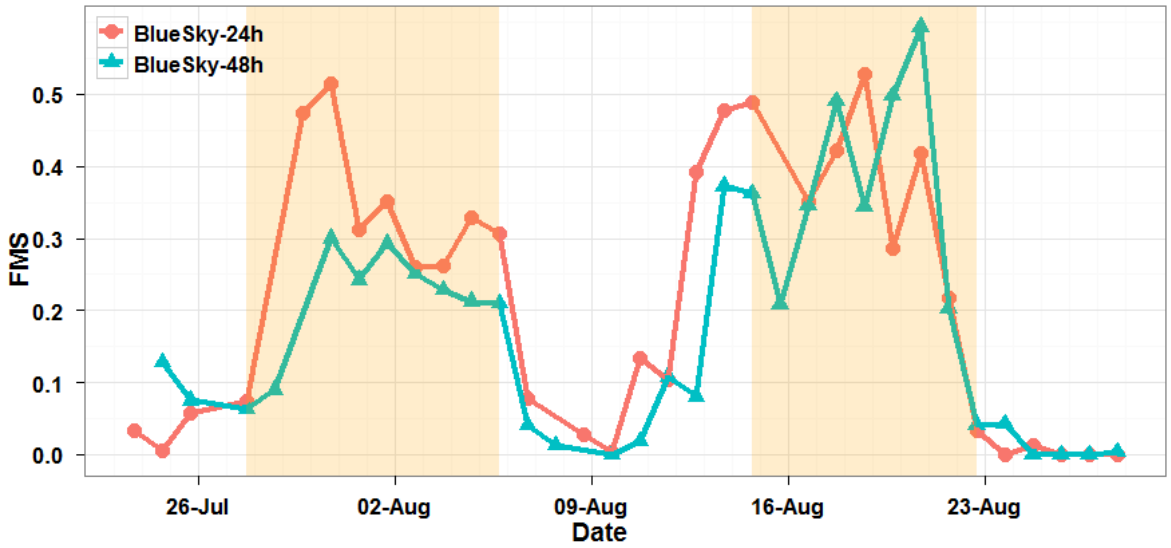

Figure 2.8 Daily Figure of Merit in space (FMS) comparing BlueSky predictions with HMS observations. The orange background indicates the major fire events during the study period. The red and blue dots are FMS computed from the BlueSky 24-hour and BlueSky 48-hour predictions, respectively.

2.2.2 Comparison between BlueSky and monitoring measurements

Table 2.3 summarizes the descriptive statistics for the $PM_{2.5}$ concentrations measured by monitors and predicted by BlueSky 24-hour or 48-hour in advance, at 36 locations in British Columbia between July 24th and August 25th, 2010. As suggested in the table, a large proportion of the BlueSky predictions were zeros (indicating no predicted smoke). Figure 2.9 shows the histogram of the $PM_{2.5}$ concentrations measured by monitors and predicted by BlueSky, excluding all of the zero values.

Table 2.3 Descriptive statistics of $PM_{2.5}$ concentrations measured by monitors and predicted by BlueSky. Mean, median, maximum (Max), minimum (Min) and standard deviation (SD) are in µg/m^3. n.valid is the number of valid records, n.zero is the number of zero values in the records.

Exposure	n. valid	n. zero	Mean	Median	Max	Min	SD
Monitor	1021	0	11.27	6.2	176.41	0.12	17.85
BlueSky-24h	1080	700	18.58	0	5483.00	0	177.87
BlueSky-48h	1050	772	7.67	0	1657.50	0	61.00

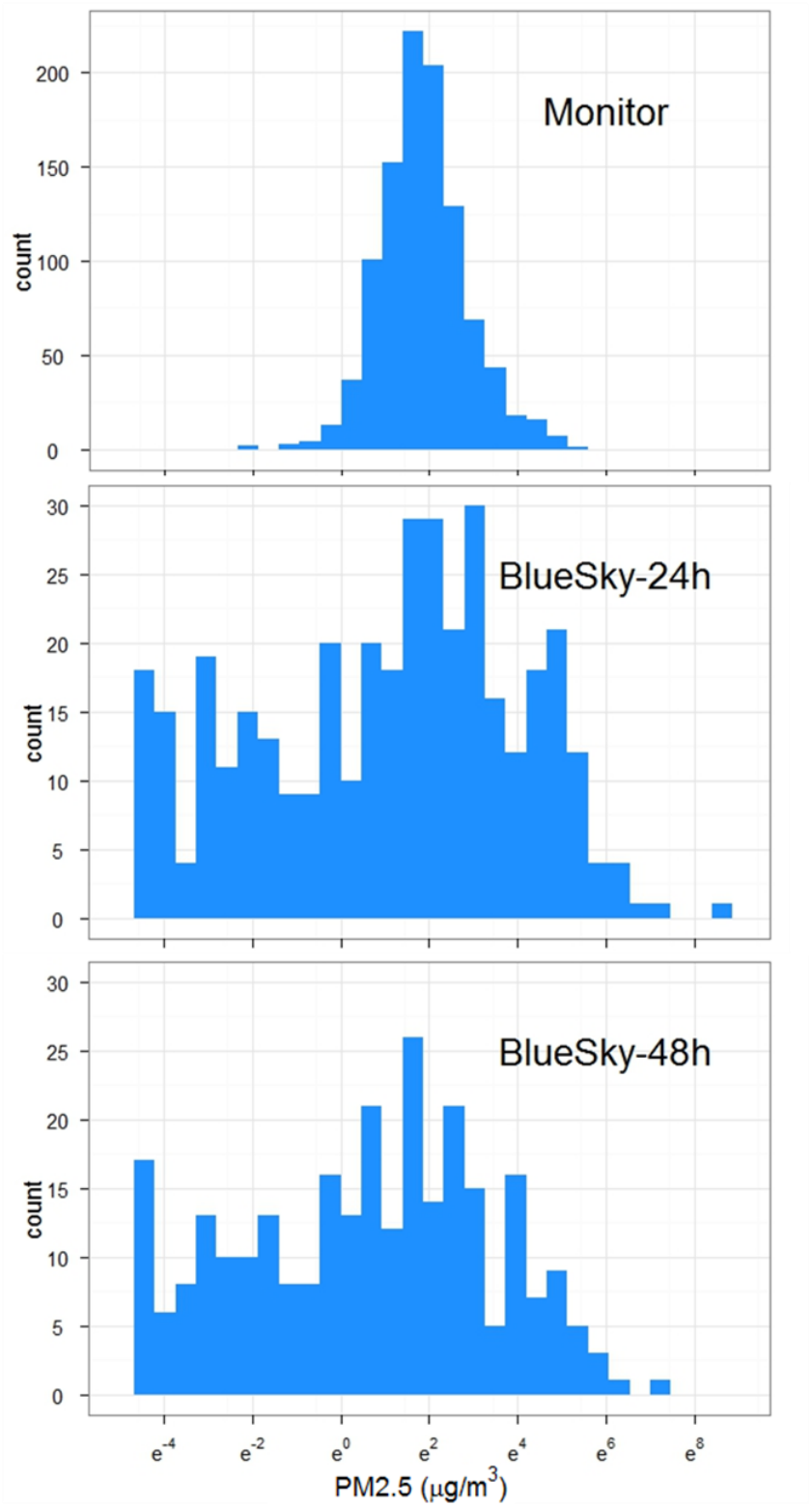

Figure 2.9 Histograms of $PM_{2.5}$ concentrations measured by monitors and predicted by BlueSky (excluding zeros).

The top figure for monitor had a different scale of y-axis from the ones for BlueSky predictions.

2.2.2.1 Global analysis

Table 2.4 presents the results of the model evaluation statistics for the global analysis, calculated with data from all times and all locations. Statistics for both the whole dataset and the dataset excluding the records with zero values in the BlueSky predictions were calculated and presented, in order to illustrate and eliminate the impact of the zero values on the results. Results show that the zero values influenced the NRMSE and FB statistics, but not the IOA and correlation statistics. All statistics indicated that BlueSky 48-hour predictions had better agreement with the monitoring measurements than the 24-hour predictions. Figure 2.11 shows two Bland-Altman plots with the 24-hour and 48-hour BlueSky predictions (excluding zeros) and monitoring data. The extreme differences came from BlueSky overpredictions that occurred more frequently in the 24-hour predictions than in the 48-hour predictions.

Table 2.4 Model evaluation statistics for global analysis with all data and data excluding records with zero BlueSky predictions.

IOA = index of agreement, r = Pearson's correlation coefficient, NRMSE = normalized root mean squared error, FB = fractional bias.

	All data included				Data excluding zero			
	IOA	r	NRMSE	FB	IOA	r	NRMSE	FB
BlueSky-24h	0.35	0.29	27.2	0.49	0.32	0.27	44.9	1.03
BlueSky-48h	0.53	0.40	18	-0.45	0.51	0.40	32.6	0.25

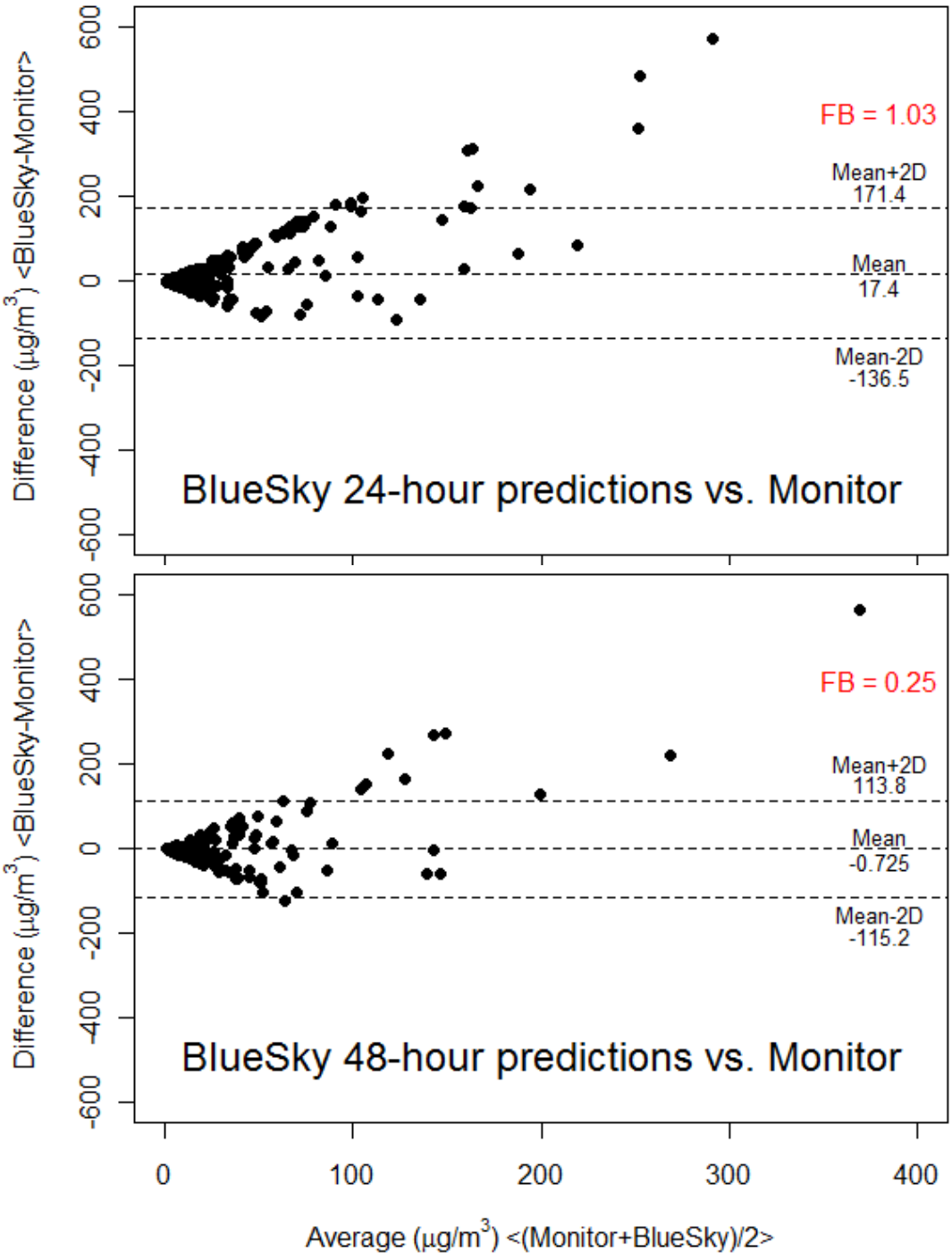

Figure 2.10 Bland-Altman plots of BlueSky 24-hour (top) and 48-hour predictions (bottom) comparing to monitoring measurements.

The x-axis is the average of BlueSky predictions and monitor measurements and y-axis is the difference between the two. The mean and confidence interval of the difference are indicated in the figures as well as the corresponding overall fractional bias (FB). Points above the zero in vertical suggest overpredictions from BlueSky compared with monitors.

2.2.2.2 Spatial analysis

In the spatial analysis, model evaluation statistics were calculated for each day using predictions and measurements from all locations. Table 2.5 summarizes the averages of these daily statistics. The 24-hour and 48-hour predictions had similar averaged IOA and correlations, but different NRMSE and FB values. Figures 2.11 to 2.14 show plots of the statistics calculated from all selected locations on each day. Variability was clear in the IOA (Figure 2.11) and the correlation coefficients (Figure 2.12) during the study period. Overall, better IOA and correlation values were observed in the middle of the fire periods (time periods with orange background in the figure), and this trend was more consistent during the second fire period. Several extremely large values of NRMSE were observed (Figure 2.13). When extreme values (greater than 100%) were excluded, the range of NRMSE was between 20% and 80%. Days with extremely high NRMSE will be described in the following paragraph. In Figure 2.14, the FB values are mostly negative, indicating the BlueSky predictions were smaller than the measurements during periods without major fire events. This is reasonable considering that BlueSky predictions at most locations were zero, while monitors were still detecting $PM_{2.5}$ from other local sources. In the middle of the fire period, FB tended to be positive or negative to a lesser extent. Overall, all of the statistics suggested that BlueSky produced forecasts in better agreement with monitoring measurements in the middle of the major fire periods. More frequent and large-scale overpredictions from BlueSky were observed.

Table 2.5 Averages (ranges) of the model evaluation statistics from spatial analysis.

Averages (ranges) of the statistics calculated from BlueSky predictions and monitoring measurements at different locations on each day.

	IOA	r	NRMSE (%)	FB
BlueSky-24h	0.40 (0.01-0.84)	0.31 (-0.37-0.87)	112 (20-1249)	-0.47 (-2.00-1.72)
BlueSky-48h	0.41 (0.02-0.82)	0.32 (-0.17-0.92)	66 (16-538)	-0.91 (-2.00-1.03)

According to Figure 2.13, there were six days (four days of BlueSky 24-hour predictions and two days of BlueSky 48-hour predictions) with NRMSE larger than 200%, suggesting large-scale disagreement between BlueSky predictions and monitoring measurements. Figure 2.15 and 2.16 visually compare the spatial agreement between BlueSky predictions (24-hour and 48-hour, respectively) and HMS plumes as well as monitoring data on these six days. Specifically, on most of these days, BlueSky produced smoke plumes with high concentrations in the Vancouver Coastal region, which was not reflected by monitoring measurements and HMS plumes. Several explanations are possible. Because this region is densely populated it has a dense air quality monitoring network, so disagreement between predicted and observed smoke is more likely to be captured by the analysis. At the same time, fires that develop in such a populated region are likely to be extinguished quickly, so their real impact may be much smaller than that predicted by BlueSky, which cannot account for human intervention. Finally, it could simply reflect poor BlueSky performance during that period, where the models predicted some entrainment of smoke from the layers aloft that did not actually occur.

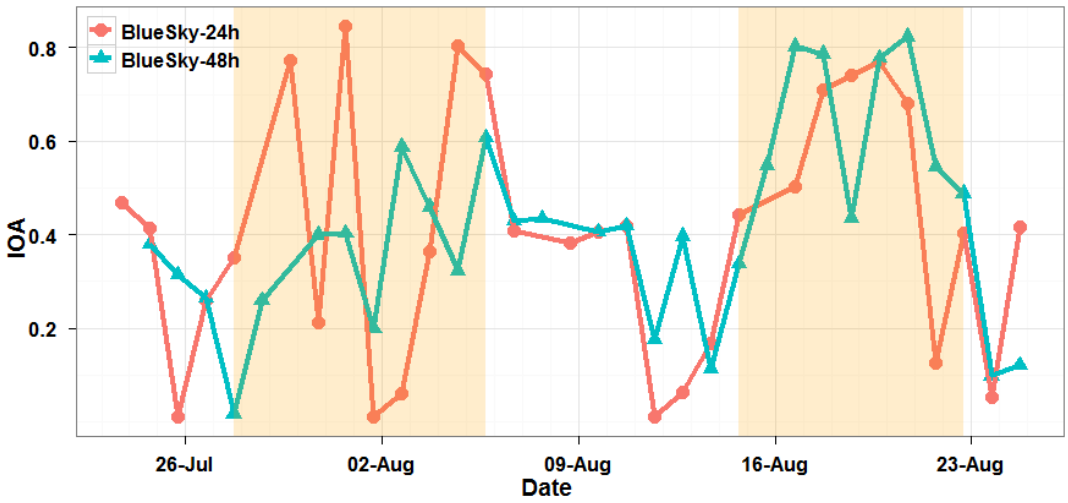

Figure 2.11 Daily index of agreement (IOA).

Orange background indicates the major fire events during the study period. Red and blue dots are IOA computed from BlueSky 24-hour and 48-hour predictions, respectively, with monitoring measurements.

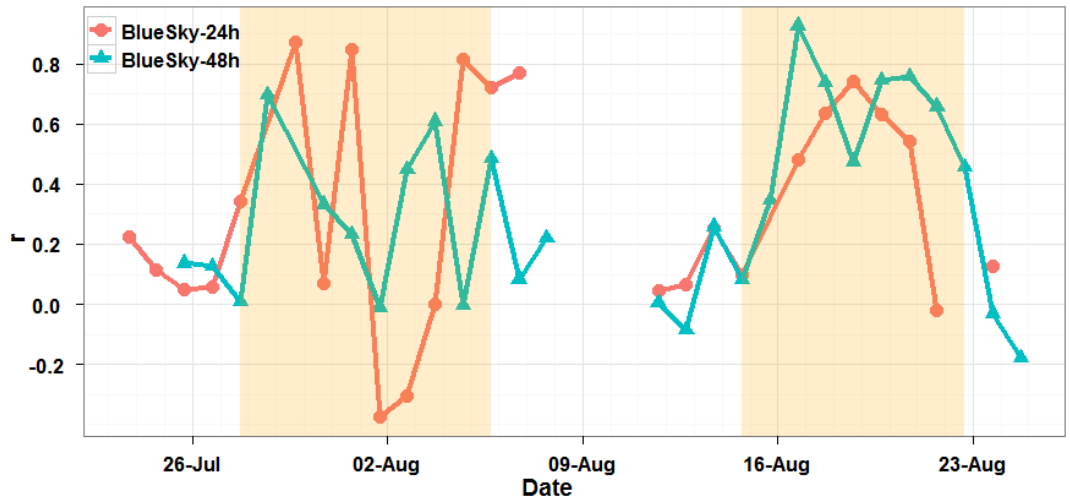

Figure 2.12 Daily Pearson's correlation coefficient (r).

Orange background indicates the major fire events during the study period. Red and blue dots are correlations computed from BlueSky 24-hour and 48-hour predictions, respectively, with monitoring measurements.

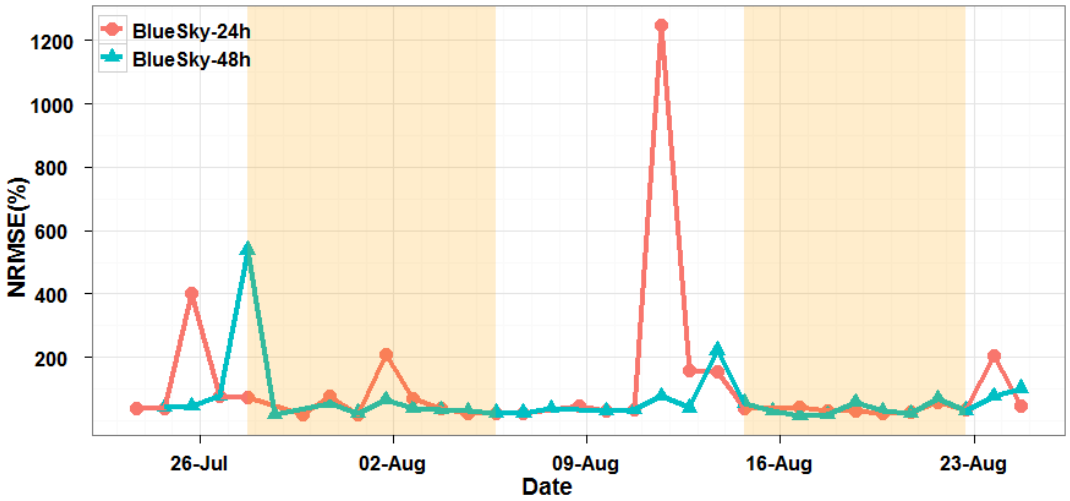

Figure 2.13 Daily normalized root mean squared error (NRMSE).

Orange background indicates the major fire events during the study period. Red and blue dots are NRMSE computed from BlueSky 24-hour and 48-hour predictions, respectively, with monitoring measurements.

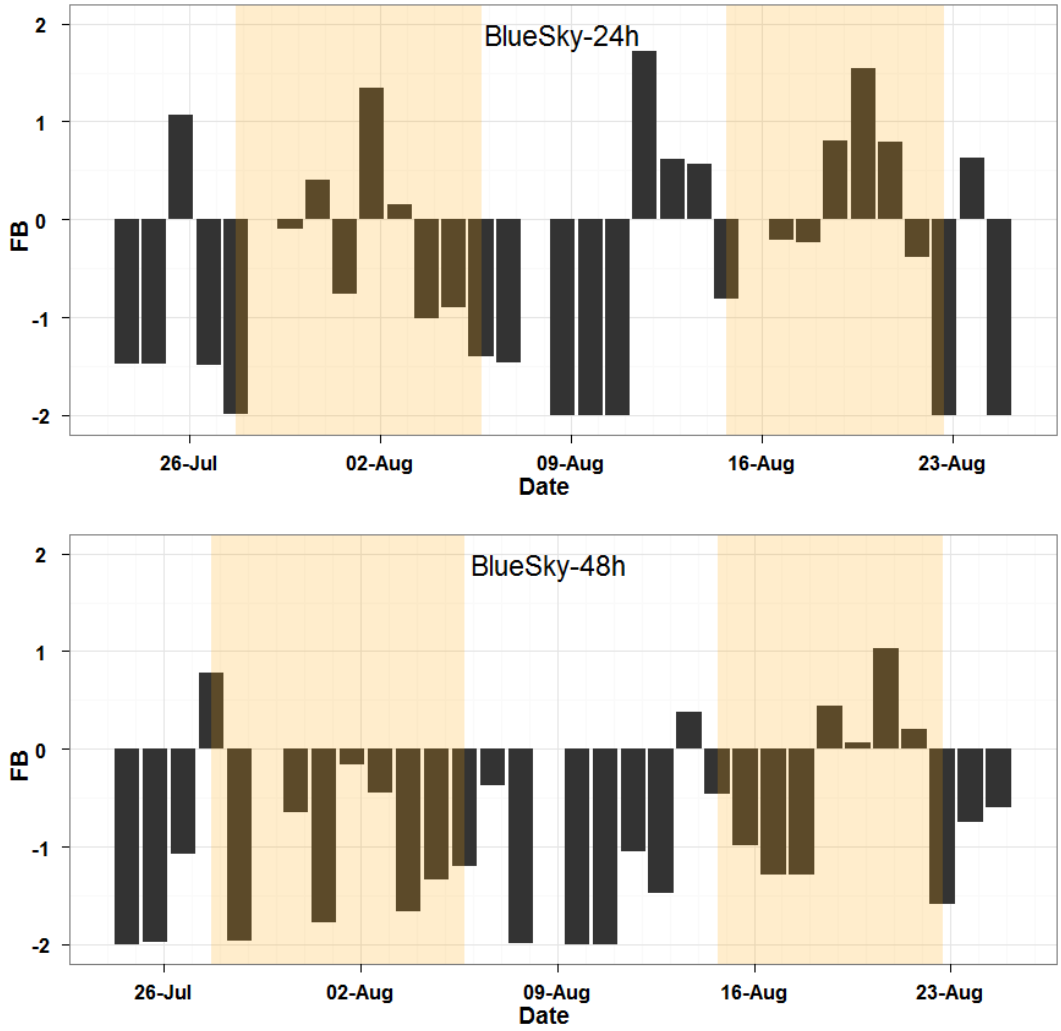

Figure 2.14 Daily averaged fractional bias (FB).

The top and bottom figures are daily FB computed from BlueSky 24-hour and 48-hour predictions, respectively, with monitoring measurements. The orange background indicates the major fire events during the study period. FB larger than 0 indicates overprediction from BlueSky and FB smaller than 0 indicates underprediction from BlueSky.

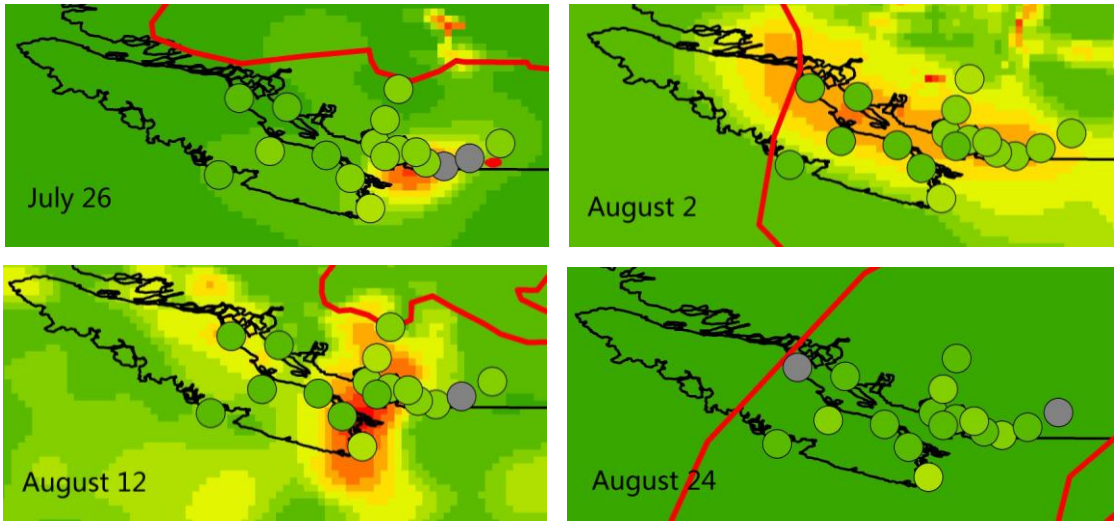

Figure 2.15 Spatial comparison of BlueSky 24-hour predictions, HMS, and monitoring outputs on days with normalized root mean squared error larger than 200%.
Colors in circles indicate concentrations measured by monitors, in the same color scale as the background of the BlueSky output rasters. Grey dots indicate malfunctioning monitors.

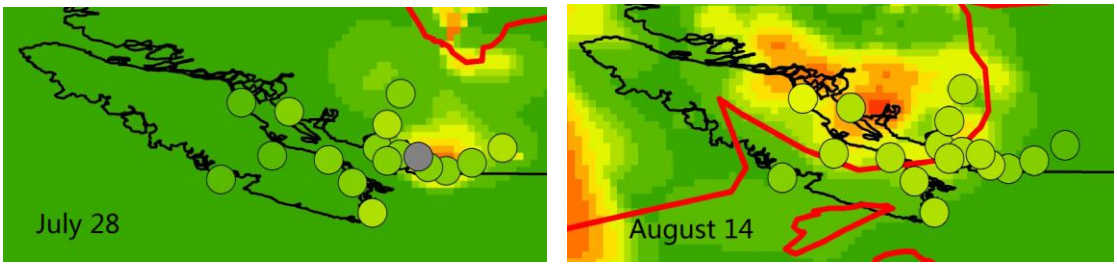

Figure 2.16 Spatial comparison of BlueSky 48-hour predictions, HMS, and monitoring outputs on days with normalized root mean squared error larger than 200%.
Colors in circles indicate concentrations measured by monitors, in the same color scale as the background of the BlueSky output rasters.

2.2.2.3 Temporal analysis

Table 2.6 summarizes the evaluation statistics calculated from the temporal analyses using all selected monitors in BC. Similar to the results of the spatial analysis (Section 2.2.2.2), improved evaluation statistics were observed from the 48-hour predictions compared with the 24-hour predictions. In addition, agreement between the monitoring data and the BlueSky output was more variable for the 24-hour predictions than for the 48-hour predictions. Figures 2.17 through 2.20 show the maps of the statistics resulting from the temporal analyses. Generally better agreement was observed in the Central Interior of BC, where wildfire smoke had the most severe and lasting impacts in 2010. This pattern was more obvious with the 24-hour predictions. When referring to the distribution of FB for the 24-hour predictions in Figure 2.20 (left figure), more overpredictions were observed in the Lower Fraser Valley and South Vancouver Island regions while more underpredictions were observed in the Southern Interior.

In summary, smoke plumes predicted by BlueSky were generally smaller than those observed by HMS. The agreement between the two was comparable with other existing smoke forecasting systems and especially good agreement was observed during the middle of the fire periods. $PM_{2.5}$ predictions from BlueSky agreed well with monitoring measurements in areas severely and consistently impacted by wildfire smoke during the middle of the fire periods. BlueSky tended to overpredict high concentrations.

Table 2.6 Averages (ranges) of the model evaluation statistics from temporal analysis.

Averages (ranges) of the statistics calculated from BlueSky predictions and monitoring measurements on different days at each location.

	IOA	r	NRMSE (%)	FB
BlueSky-24h	0.27 (0-0.88)	0.11 (-0.17-0.83)	109 (24-648)	-0.25 (-1.91-1.73)
BlueSky-48h	0.46 (0.02-0.80)	0.31 (-0.36-0.86)	52 (20-224)	-1.06 (-1.97-1.30)

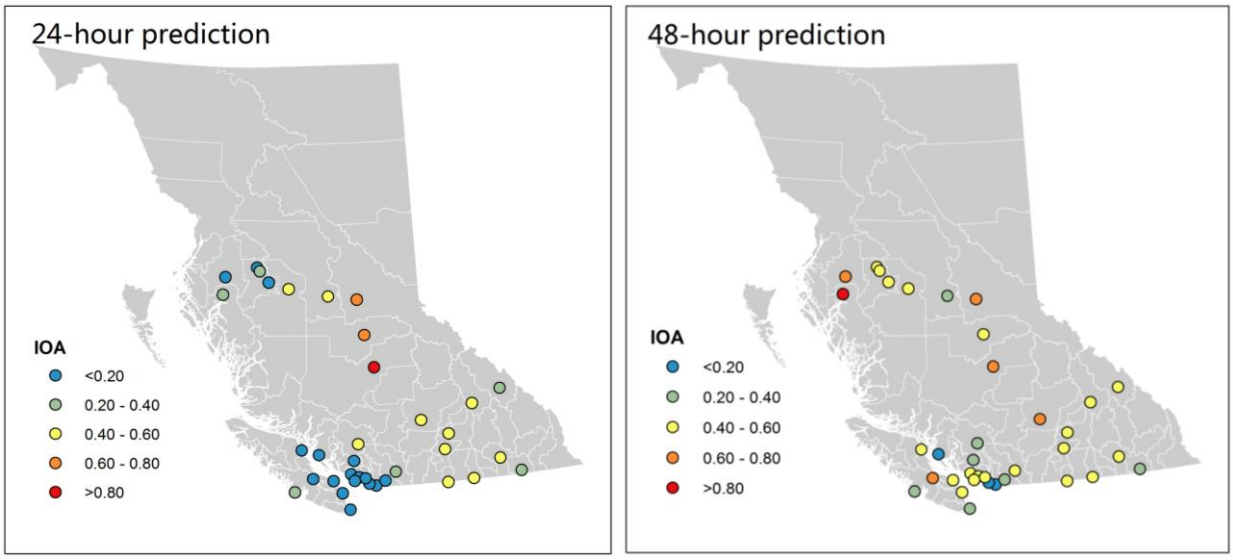

Figure 2.17 Index of agreement (IOA) from temporal analysis at different locations in British Columbia. IOA for 24-hour predictions on the left and IOA for 48-hour predictions on the right. The color of the dots corresponds to the value of IOA.

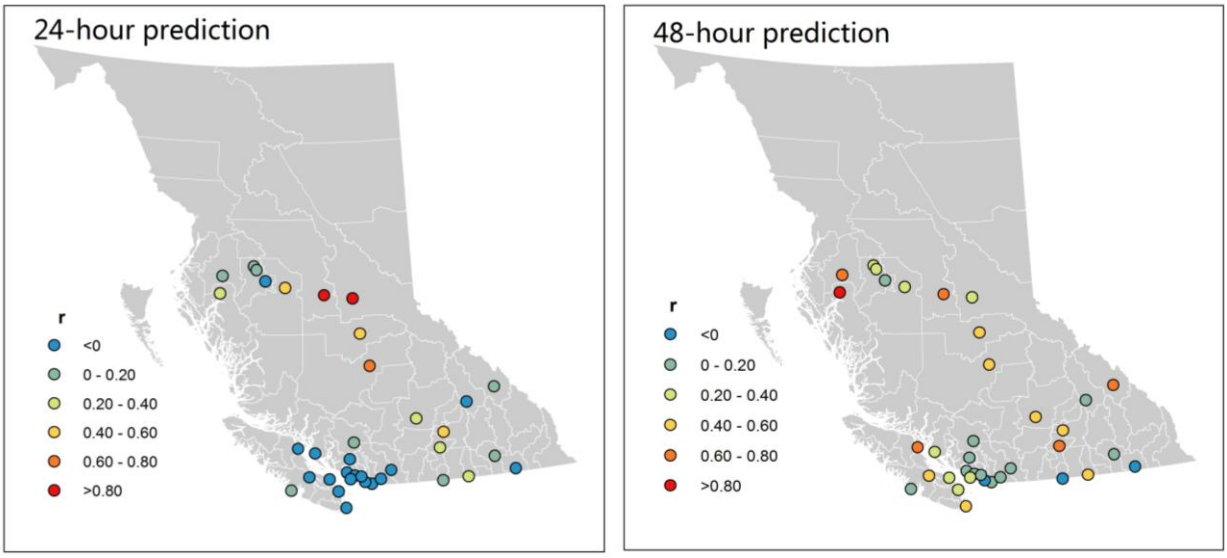

Figure 2.18 Correlation coefficients (r) from temporal analysis at different locations in British Columbia. Values of r for 24-hour predictions on the left and values of r for 48-hour predictions on the right. The color of the dots corresponds to the value of r.

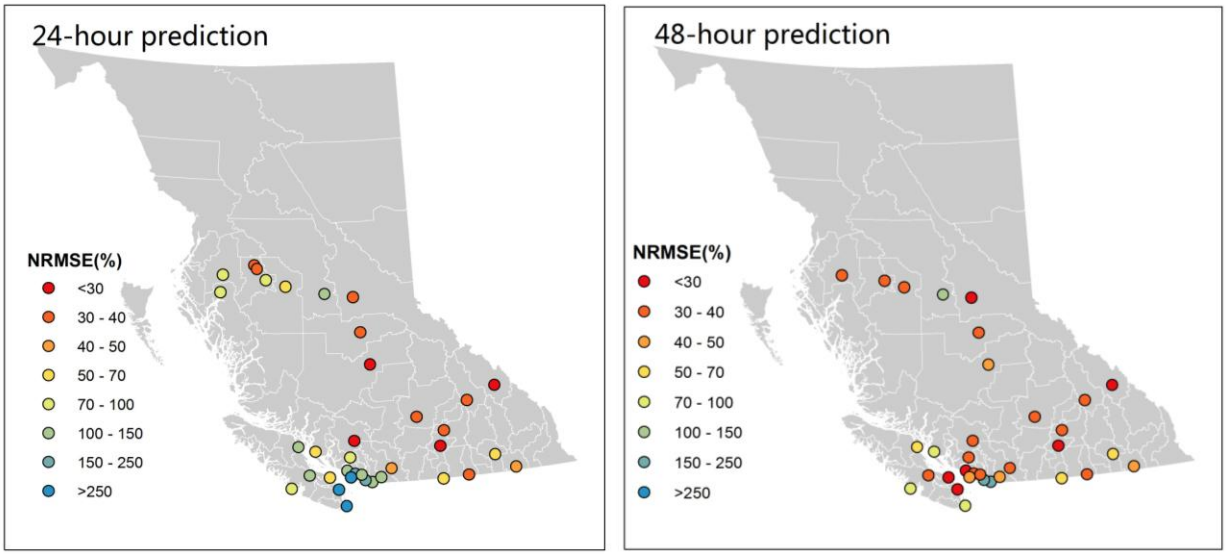

Figure 2.19 Normalized root mean squared error (NRMSE) from temporal analysis at different locations in British Columbia.

NRMSE for 24-hour predictions on the left and NRMSE for 48-hour predictions on the right. The color of the dots corresponds to the value of NRMSE.

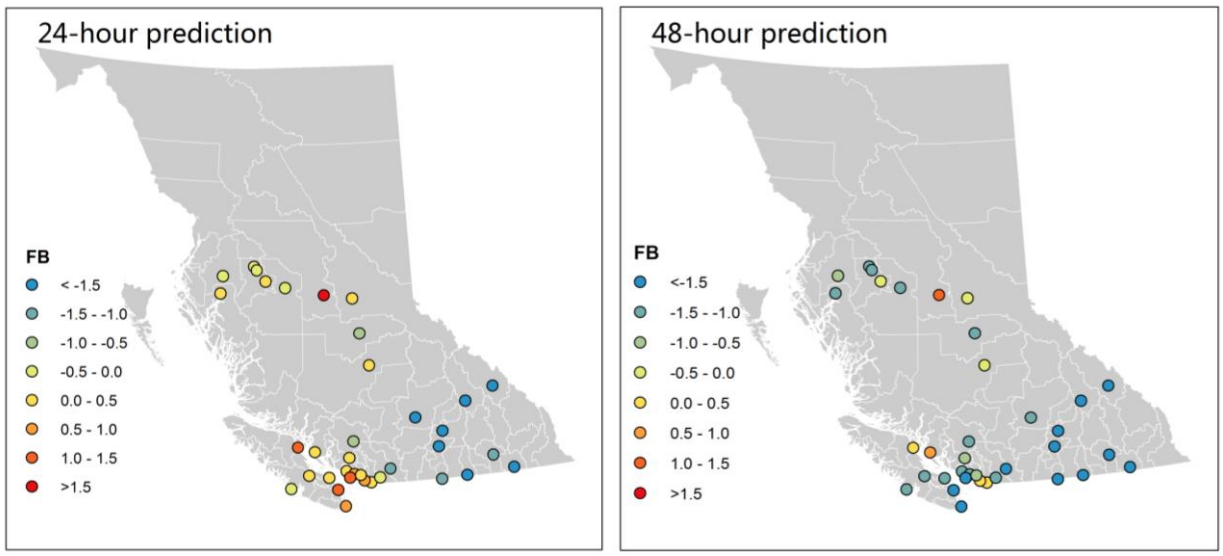

Figure 2.20 Fractional bias (FB) from temporal analysis at different locations in British Columbia.

FB for 24-hour predictions on the left and FB for 48-hour predictions on the right. The color of the dots corresponds to the value of FB.

3. Association between BlueSky predictions and respiratory health outcomes

This chapter describes the second objective of the thesis study, which was to assess the association between BlueSky predictions of $PM_{2.5}$ concentrations with respiratory health outcome indicators during the forest fire periods in 2010 summer in BC. As reference, the association between the health outcome indicators and ground-level monitoring station measured $PM_{2.5}$ concentrations as well as the smoke coverage indicated by HMS images are also presented. This is the first study to relate wildfire smoke predictions to public health outcomes of any kind.

3.1 Methods

This section describes (1) the methods used to collect the respiratory health outcome data, (2) the methods used to assign exposure variables from the BlueSky model, monitoring measurements, and HMS images to each of the local health areas, and (3) the statistical analyses applied to assess the association between exposure and health outcomes.

The first step was to gather all data needed: (1) health outcome data, including salbutamol dispensations for respiratory symptoms and MSP claims of physician visits for asthma; (2) exposure data, including BlueSky predicted and HMS observed smoke plume coverage as well as BlueSky predicted and monitoring measured $PM_{2.5}$ concentrations assigned to each LHA; and (3) data for other covariates included in the statistical model.

A total of twelve Poisson regressions were conducted to estimate the independent fixed effects of the six exposure variables (three continuous and three binominal) on two health outcome variables. In addition, four other covariates were included in each of the regressions.

The coefficients of the exposure variables from the regressions were used to compute the relative risks of the health outcome from the increased exposure.

The following sections will describe these processes in detail.

3.1.1 Health outcome data

Data for two respiratory health outcome indicators were retrieved from Environmental Health Services in the British Columbia Center for Disease Control (BCCDC):

(1) Medication dispensations, the daily counts of salbutamol sulfate prescriptions dispensed in each of the 85 LHAs with available data in BC (see Figure 3.1). Salbutamol sulfate is commonly used for the relief of bronchospasm caused by asthma or other chronic airways diseases, and is usually delivered through an inhaler. Its daily counts during the study period were extracted from the BC PharmaNet database. In BC, the law requires every prescription dispensed in the province be recorded in this database.

(2) Physician visits, the daily counts of medical service plan (MSP) claims of general services for asthma (ICD code 493) within each of the 73 LHAs with available data in BC (see Figure 3.1). Data from LHAs on the Vancouver Island were not included in the dataset because the Vancouver Island Health Authority chose not to participate in the surveillance program for which the data were collected. This region was not heavily affected by smoke during the summer of 2010.

These daily health outcome counts were divided by the total population of the corresponding LHA, resulting in the daily health outcome rates for each of the LHAs. The total population for each LHA was calculated from the Dissimilation Area population counts obtained from the 2006 census collected by Statistics Canada.

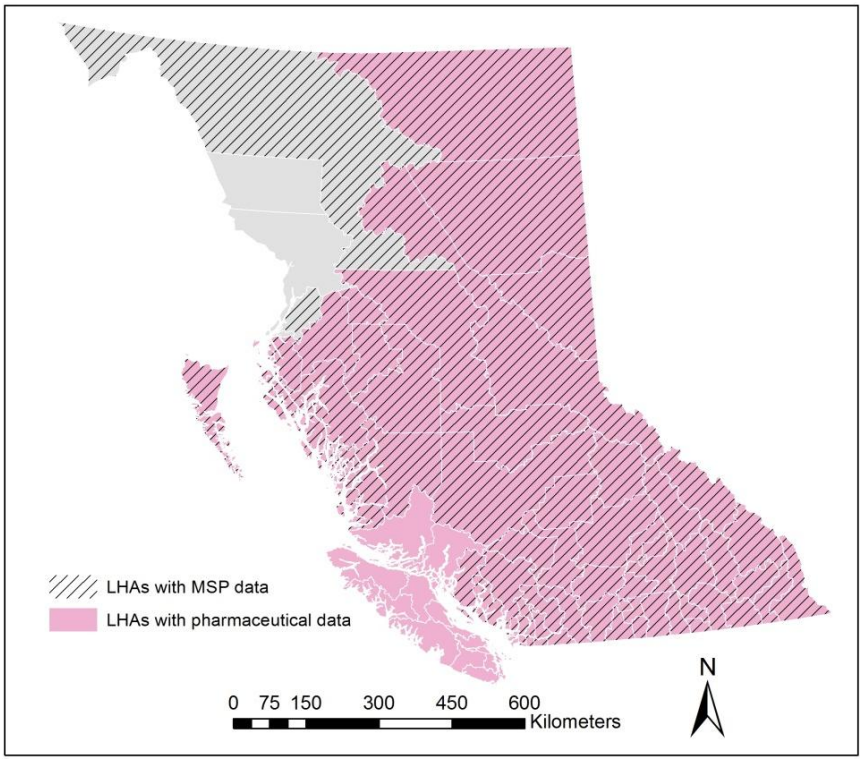

Figure 3.1 Local health areas (LHA) with pharmaceutical and MSP data.
Crosshatched areas are LHAs with pharmaceutical data and areas in pink are LHAs with MSP physician visit data.

3.1.2 Exposure data

A total of six exposure variables (three binary and three continuous) were derived from the BlueSky predictions, monitoring station measurements, and HMS images. The collection of these data has been described previously in Section 2.1.1 and this section describes the method used to assign values to LHAs.

Within each LHA, there are different numbers (ranging from 3 to 474) of dissemination area (DA) centroids with population records (see Figure 3.2). These population centroids were the units used to assign exposure values to the LHAs.

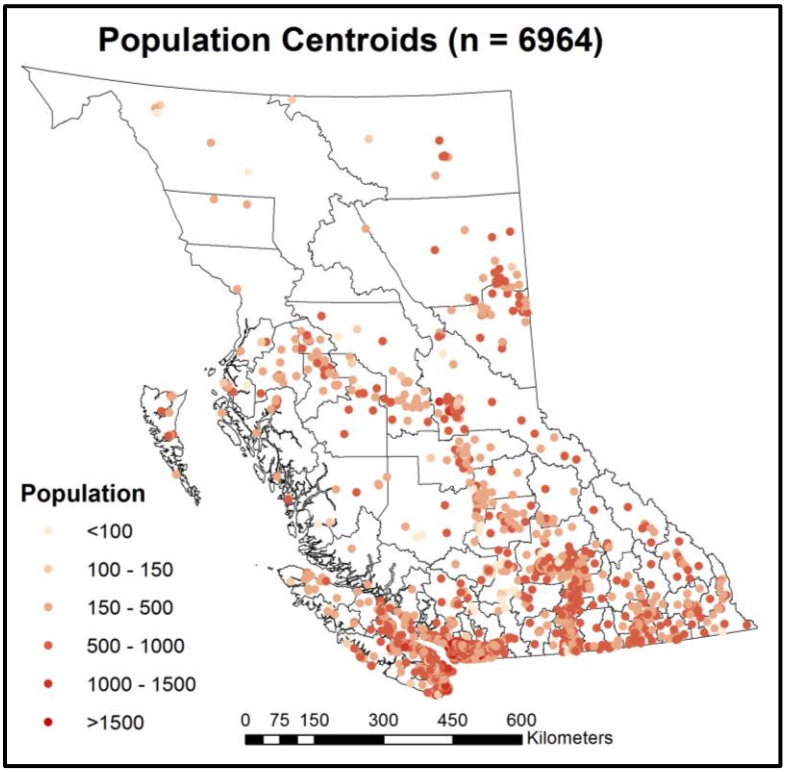

Figure 3.2 Population centroids in British Columbia.

Two continuous variables were created from the BlueSky predictions (BlueSky 24-h and BlueSky 48-h). The daily average BlueSky prediction raster was overlaid with the population centroids, and the $PM_{2.5}$ values of the pixels underlying the DA centroids were extracted in ArcMap. Next, a population weighted average of the $PM_{2.5}$ predictions was calculated for the LHA using Equation 3.1:

$$\bar{x} = \frac{x_1 p_1 + x_2 p_2 + \cdots + x_n p_n}{p_1 + p_2 + \cdots + p_n} \qquad \text{Equation 3.1}$$

where $\bar{x}$ is the population weighted average prediction assigned to the LHA, x_n is the concentration assigned to the DA centroid and p_n is the population of the corresponding DA.

In addition, two binary variables (BlueSky-cover-24h and BlueSky-cover-48h) were derived from the BlueSky predictions. LHAs with a population weighted average BlueSky prediction (24-hour or 48-hour) larger than zero on each day were assigned a value of 1 and otherwise a value of 0. These two variables described if any population in the specific LHA on the specific day was covered by the smoke plume predicted by BlueSky.

A continuous variable (Monitor) was derived from monitoring $PM_{2.5}$ measurements. Each of the population centroids was assigned the daily $PM_{2.5}$ concentrations from the nearest monitoring station out of the 55 monitoring stations in British Columbia, described in Section 2.1.2. The calculations were made using the "near" function of ArcMap. Then a population weighted average for each LHA was calculated using the Equation 3.1.

A binary variable (HMS) was derived from the HMS smoke plume images. The HMS smoke plume images were overlaid on the study area with the DA population centroids. By intersecting these layers in ArcMap, the population centroids that were covered by the HMS could be identified. Any LHA with any DA population centroid that fell within the smoke plume received a value of 1 and otherwise it received a value of 0. This binary variable described if any population in the specific LHA on the specific day was covered by the smoke plume observed by HMS.

3.1.3 Other covariates

In addition to the exposure variables and health outcome indicators, the following covariates were included in the analyses:

(1) Daily maximum temperature. Exposure to high temperature has been associated with mortality and morbidity for respiratory causes. (Michelozzi et al., 2009; Shao et al., 2009) As

hot and dry weather is one of the contributors for intense wildfire activity, wildfire seasons are typically accompanied with high temperatures. Thus, we need to account for the potential confounding effects by introducing this covariate in the statistical model. Daily maximum temperature records were retrieved from the BC Ministry of Environment website and the measurements were available in 56 locations in BC (see Figure 3.3). All of the DA population centroids were assigned the daily maximum temperature values from the nearest meteorological monitor. A population weighted daily maximum temperature for each LHA was calculated using the Equation 3.1.

(2) A day-of-week indicator. A range of values from 1 to 7 were assigned to Monday to Sunday (Monday=1, Tuesday=2, etc.) for all outcomes. As most of the pharmacies and clinics were closed during weekends, a sharp decrease in counts of medication dispensations and general physician visits was observed. Including this indicator in the model can account for the weekday/weekend effect.

(3) A holiday indicator. Dates of public holidays were assigned a value of 1 and otherwise a value of 0. Similar to the day-of-week indicator, including a holiday indicator can account for the influence from sharp decrease in health outcome counts on holidays, when most pharmacies and clinics are closed.

(4) A time-trend indicator "number of week". This covariate was applied to account for unspecified time-varying trend, if there was any. The first week of the study period was assigned a value of 1 and the second week was assigned a value of 2, etc.

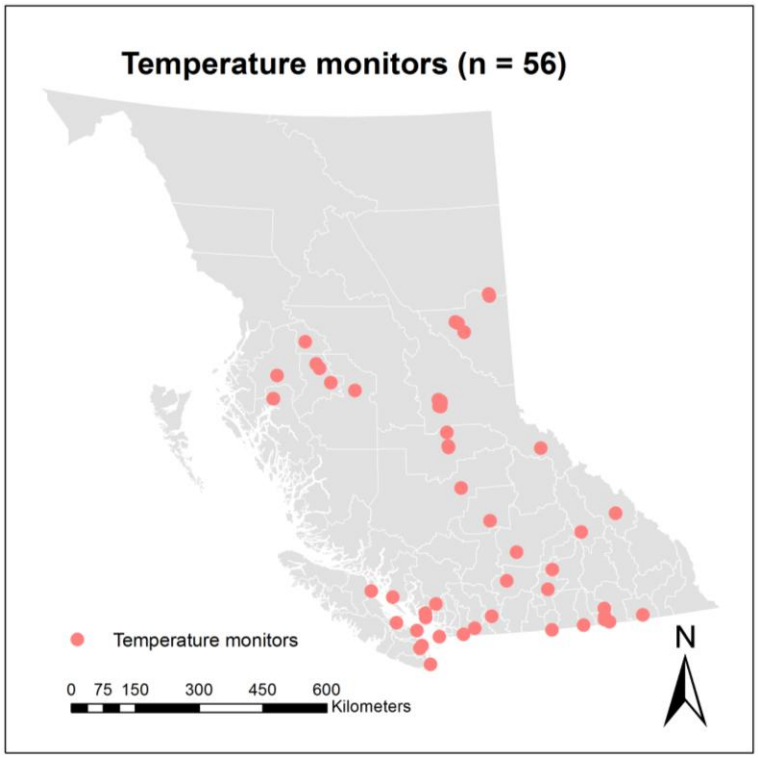

Figure 3.3 Locations of temperature monitors used in the study.

3.1.4 Statistical analyses

Twelve Poisson regressions were constructed with the six exposure variables (BlueSky-24h, BlueSky-48h, Monitor, BlueSky-cover-24h, BlueSky-cover-48h and HMS) as independent variables and the two health outcome measures (Medication dispensation rates and Physician visit rates) as dependent variables. As the health outcomes included in the analyses came from different LHAs on different days, those that came from the same LHA might be autocorrelated. To account for this correlation within individual LHAs, parameters in the regression models were calculated with generalized estimation equation (GEE) using the GEE package in R, assuming an exchangeable correlation structure. Equation 3.2 illustrates the model, where μ_{it} is the count of the health outcome for LHA *i* on day *t*; p_i is the

2006 census population of LHA *i*; β_0 is a fixed intercept; x_{it} is the exposure for LHA *i* on day *t*; K_{it} is the maximum temperature for LHA *i* on day *t*, D_t is the day of week on day *t*, H_t is the holiday indicator value on day *t* and N_t is the number of week on day *t*:

$$\text{Log}(E(\mu_{it}/p_i)) = \beta_0 + (\beta_1 z_{it} + \beta_2 D_t + \beta_3 H_t + \beta_4 N_t) + \beta x_{it} \qquad \text{Equation 3.2}$$

The coefficient β of exposure variable x_{it} was used to calculate the relative risk of the health outcome.

3.2 Results

3.2.1 Descriptive statistics

Monitoring measured population-weighted 24-hour $PM_{2.5}$ concentrations for each LHA ranged from 0.025 to 176.4 μg/m^3 during the study period (July 24 – August 29). Over all LHAs during the study period, the mean exposure was 10.0 μg/m^3, with an interquartile range between 3.0 and 10.1 μg/m^3. Population-weighted 24-hour $PM_{2.5}$ concentrations for each LHA predicted by BlueSky 24 hours in advance ranged from 0 to 2334 μg/m^3. The mean was 10.6 μg/m^3 with an interquartile range between 0 and 0.4 μg/m^3. Population-weighted 24-hour $PM_{2.5}$ concentrations for each LHA predicted by BlueSky 48 hours in advance ranged from 0 to 988 μg/m^3. The mean was 4.0 μg/m^3 with an interquartile range between 0 and 0.1 μg/m^3. The distribution of predictions from BlueSky was highly skewed due to the large number of zero values in the output. This distribution is typical for air quality model outputs (Mosca et al., 1998), especially for models that only account for one kind of source (only wildfire smoke in our case). At the same time the small fraction of very large values had great impact on the mean and they are expected to impact the estimate in the regression analysis. This impact will be further discussed in Section 4.2.

The number of days covered by smoke plumes observed by HMS for LHAs ranged from 6 to 26 (out of 35), with a mean of 15.8 days (Figure 3.4). The number of days covered by smoke plumes predicted by BlueSky 24-hours in advance ranged from 5 to 26 (out of 33), with a mean of 13.2. The number of days covered by smoke plumes predicted by BlueSky 48-hours in advance ranged from 3 to 24 (out of 34), with a mean of 11.7. LHAs that were more constantly impacted by smoke plumes were in the northern and central interior regions.

Table 3.2 summarizes the overall outcome rates and outcome rates on weekdays and weekends/holidays for respiratory medication dispensation and physician visits during the study period. As expected, both outcome rates had sharp decreases during weekend and holidays compared with weekdays. A large range of outcomes rates was observed across different LHAs. This might indicate potential influences from the variation in demographics, socioeconomic statuses, and the availability of health facilities in different LHAs, as indicated by the BC Health Atlas. It could also indicate their differences in the exposures to environmental hazards (such as wildfire smoke) during the study period.

Table 3.1 Summary of health outcome rates.

Outcome rates (events per 100 000 person-days) in British Columbia during the 37-day study period, presented in categories of weekday and weekend/holiday.

Categories	Medication dispensation		Physician visits	
	Overall rate	Range of LHA rates	Overall rate	Range of LHA rates
Overall	34.0 (n=56991)	(17.7 - 72.2)	9.3 (n=13080)	(2.7 – 21.1)
Weekday	42.7	(21.1 – 105.7)	12.3	(0 – 29.2)
Weekend & holiday	18.0	(0 – 31.0)	3.9	(0 – 23.0)

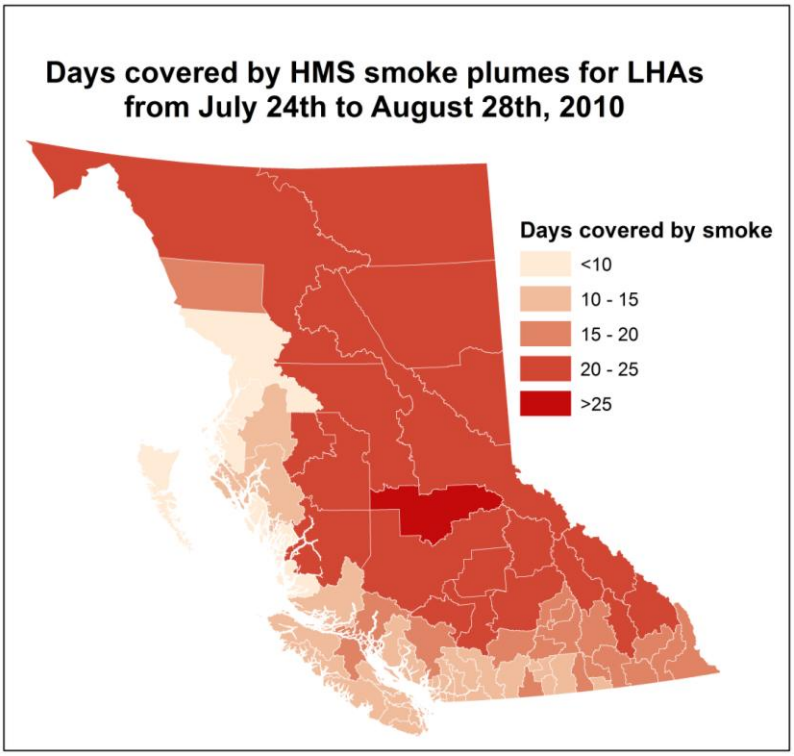

Figure 3.4 Number of days covered by HMS smoke plumes for LHAs in British Columbia during the study period.

3.2.2 Association between exposure and outcome

Table 3.3 summarizes the relative risks (RRs) associated with 30μg/m^3 increase in Monitor, BlueSky-24h and BlueSky-48h (the three continuous exposure variables), calculated from all of the LHAs with available data, as well as a subset of LHAs that had sufficient cases (mean daily asthma visits>2 and medication dispensation >5). As some of the LHAs had very small daily records of health outcome events, they might not be sufficient to reflect the impact of the forest fire smoke (or any other air pollutants) which is typically associated with small relative risks, requiring larger populations to detect. Figure 3.5 visually illustrates the RRs from all LHAs. Most of the mean and the lower bound of the RRs were greater than 1.0,

indicating significant associations between increased exposures and health outcomes. The BlueSky 24-hour predictions had smaller RRs than the 48-hour predictions, and both BlueSky predictions had smaller RRs than monitor measurements. There was no significant difference between the results from all LHAs and the subset of LHAs.

Table 3.4 summarizes RRs associated with HMS, BlueSky-cover-24h and BlueSky-cover-48h (the three binary exposure variables), calculated from all LHAs and the subset of LHAs. Figure 3.6 visually illustrates the RRs calculated from all LHAs. Most of the mean and the lower bound of the RRs were greater than 1 from the results of all LHAs. However, results from the subset of LHAs indicated insignificant association between all exposure measures and physician visits with large confidence intervals. The BlueSky-cover-48-h had an RR essentially the same as HMS, and slightly larger than the BlueSky-cover-24h.

The Cariboo-Chilcotin local health area (LHA27) was covered by smoke plumes for the longest time among all of the LHAs during the study period. Figure 3.7 plots of the daily medication dispensation counts and physician visits against the $PM_{2.5}$ concentrations measured by monitor and predicted by BlueSky plots in LHA27. It highlights the clear temporal relationship between the exposures and health outcomes. The peaks of the exposure coincide with the peaks of the health outcomes. Note that there were frequent missing values in monitoring measurements, especially in the middle of a fire event, mostly due to the malfunction of the monitors when confronted with extreme PM concentrations from wildfires.

In summary, BlueSky predictions, monitoring measurements and HMS smoke plume coverage were significantly associated with medication dispensations and physician visits for respiratory diseases. In areas consistently impacted by wildfire smoke, there was a clear temporal relationship between BlueSky predictions the respiratory health outcomes.

.

Table 3.2 Summary of results for continuous exposure variables.

RRs (95% Confidence intervals) associated with 30μg/m^3 increase in monitor measured and BlueSky predicted $PM_{2.5}$ concentrations for the two health outcomes (n indicates the number of LHAs included).

	All available LHAs		Subset of LHAs*	
	Physician Visits (n = 73)	Medication Dispensations (n = 85)	Physician Visits (n = 37)	Medication Dispensations (n = 58)
Monitor	1.07 (1.00 - 1.15)	1.12 (1.08 – 1.15)	1.04 (0.98 – 1.11)	1.11 (1.07 – 1.15)
BlueSky-24h	1.01 (1.00 - 1.02)	1.01 (1.00 – 1.01)	1.01 (1.00 – 1.02)	1.01 (1.00 – 1.02)
BlueSky-48h	1.04 (1.01 – 1.07)	1.04 (1.02 – 1.05)	1.04 (1.02 – 1.07)	1.04 (1.02 – 1.05)

* Subset of LHAs with mean daily asthma visits>2 and medication dispensation >5.

Table 3.3 Summary of results for binominal exposure variables.

RRs (95% Confidence intervals) associated with being covered by smoke plumes observed by HMS and predicted by BlueSky for the two health outcomes.

	All available LHAs		Subset of LHAs*	
	Physician visits	Medication dispensation	Physician visits	Medication dispensation
HMS	1.09 (1.00 – 1.18)	1.09 (1.04 – 1.13)	1.07 (0.97 – 1.18)	1.08 (1.03 – 1.12)
BlueSky-cover-24h	1.00 (0.93 – 1.06)	1.03 (1.00 – 1.07)	0.98 (0.90 – 1.06)	1.03 (0.99 – 1.06)
BlueSky-cover-48h	1.09 (1.03 – 1.17)	1.07 (1.03 – 1.11)	1.07 (0.99 – 1.16)	1.07 (1.03 – 1.11)

* Subset of LHAs with mean daily asthma visits>2 and medication dispensation >5.

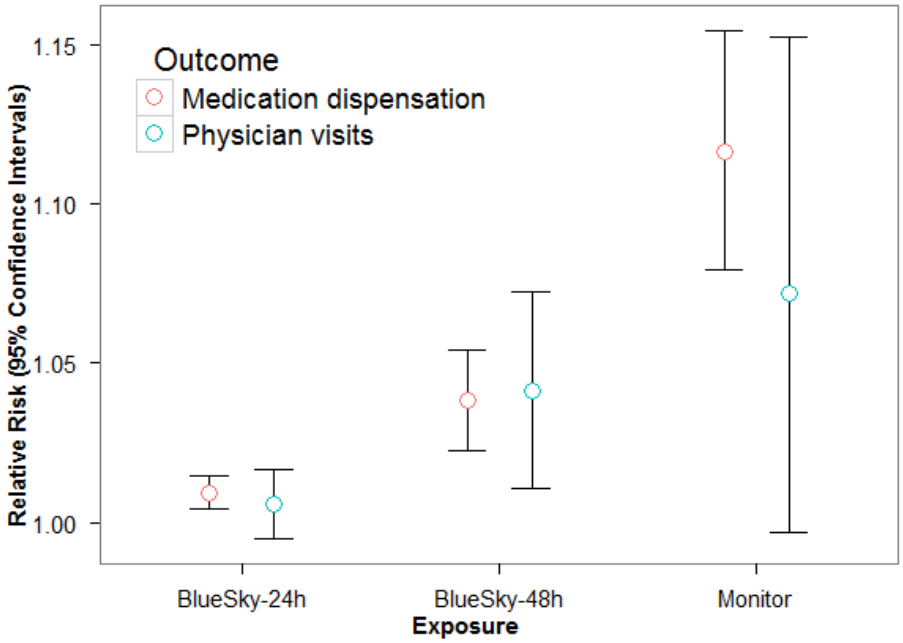

Figure 3.5 Relative risks (RRs) for physician visits and medication dispensations associated with 30µg/m^3 increase in measured and predicted $PM_{2.5}$ concentrations.

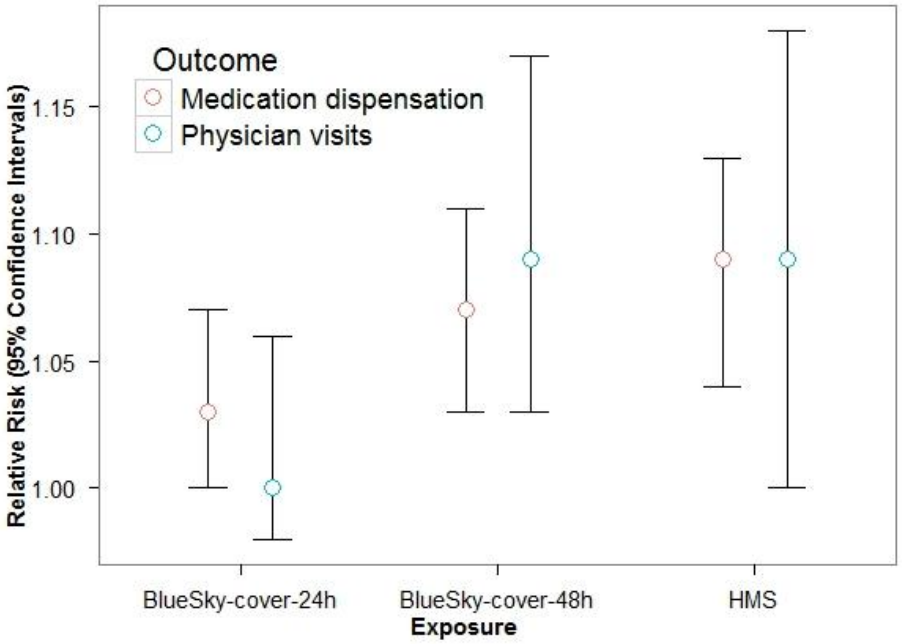

Figure 3.6 Relative risks (RRs) for physician visits and medication dispensations associated with being covered by observed and predicted smoke plumes.

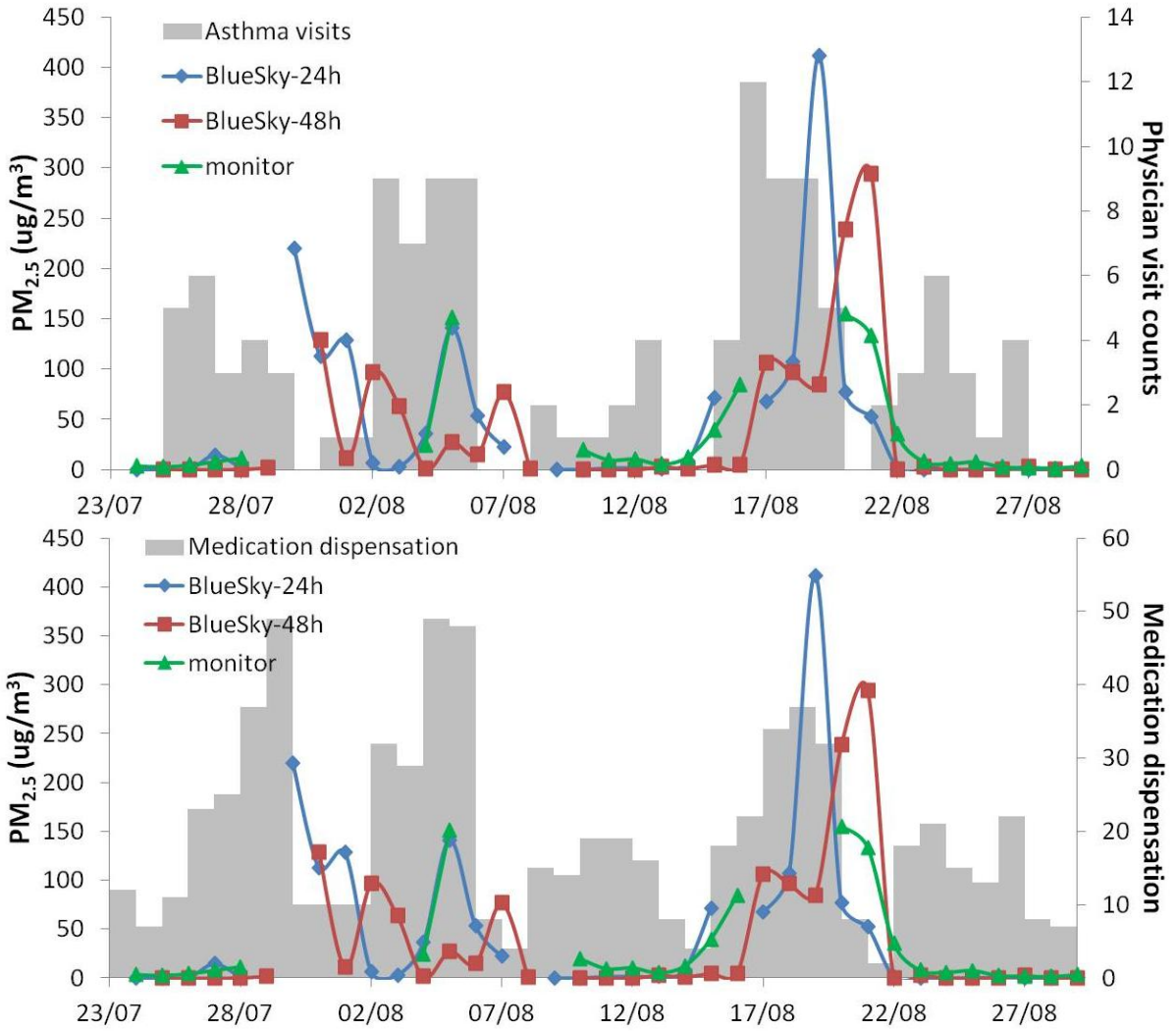

Figure 3.7 Asthma physician visit counts (top figure) and medication dispensation (bottom figure) vs. $PM_{2.5}$ concentrations from BlueSky 24-hour, 48-hour predictions and monitoring measurements in LHA27 (Cariboo-Chilcotin).

4. Discussion

The BlueSky model performance evaluation in Chapter 2 found that BlueSky predicted smaller smoke plumes within the HMS observed plumes during the intense fire periods. On the other hand, it predicted $PM_{2.5}$ concentrations comparable with monitor measurements in the middle of the fire period and in areas consistently impacted by wildfire smoke. More frequent and larger-scale overpredictions were observed in the magnitude of $PM_{2.5}$ concentrations.

Chapter 3 found significant association between BlueSky predictions and health outcomes. A 30μg/m^3 increase in BlueSky 24-hour $PM_{2.5}$ predictions was associated with 1% increase in medication dispensations and physician visits for asthma. The same increase in 48-hour predictions was associated with 4% increase in both medication dispensations and physician visits for asthma. The relative risks are smaller than those associated with monitor observed $PM_{2.5}$. On the other hand, smoke plume coverage predicted by BlueSky was associated with relative risks comparable with those estimated for smoke plumes observed by HMS.

4.1 Model performance evaluation

During the study period, the agreement between smoke plumes predicted by BlueSky and observed by HMS compared well with those reported elsewhere for other smoke forecasting systems. The FMS scores between the BlueSky 24-hour predictions and HMS ranged from 0 to 0.59 with a mean of 0.18. These scores were slightly better than the results from the Stein et al. (2009) for their evaluation of the US NOAA smoke forecasting system (SFS), where the FMS scores during three fire events between the NOAA SFS 24-hour predicted

and HMS observed plumes ranged from 0.02 to 0.40, with a mean of 0.14. As illustrated in Figure 2.9, the HMS produced larger plumes than BlueSky most of the time, similar to the evaluation of the European Fire Assimilation System (FAS) by Sofiev et al. (2009), where the predicted plumes were generally less efficiently dispersed than the ones observed by MODIS. One possible explanation is that HMS was measuring $PM_{2.5}$ in the total column of the atmosphere while BlueSky predicted only the ground-level $PM_{2.5}$. Because smoke dispersed at any height of the atmosphere could be captured by HMS as the observed smoke plumes, it was reasonable that they were larger than those predicted by BlueSky, which could only capture ground-level smoke. Also, the uncertainty in the BlueSky prediction for several elements, such as the emissions rates, injection height and meteorological parameters, could result in errors in smoke plume location and size. As BlueSky could only predict smoke from wildfires located within its domain, it was not able to capture smoke transported from regions like the southern United States and Asia.

Comparison between the BlueSky predicted and surface monitor observed $PM_{2.5}$ concentrations indicated an overall correlation of 0.29 (Table 2.5). This result compared well with correlations of 0.3 and 0.5 between predictions from the two branches of the European FAS and the MODIS observations (Sofiev et al., 2009). Generally, stronger agreement was observed during the peaks of major fire events and in areas consistently covered by smoke plumes. Significant disagreement was observed in the densely populated Vancouver Coast region, which was only mildly impacted by wildfire smoke in 2010. Similarly, larger relative disagreement was observed for the European FAS in West Europe where anthropogenic emissions were more influential than the impact of fire smoke. This is understandable because monitoring stations measure PM from all sources while the smoke forecasts predict

PM from wildfires only. In areas not heavily and consistently impacted by wildfire smoke, most of the predictions will be zeros, while monitors can still measure PM from other sources, resulting in significant overall disagreement between predictions and measurements. The inability for surface monitors to measure PM from a specific source prevents us from reliably evaluating the BlueSky predictions in areas where wildfire smoke is not the dominant source of PM.

The major differences between values predicted by BlueSky and observed by monitor were driven by the overpredictions from BlueSky, which happened more often and to a much larger extent than underpredictions. A similar finding was also reported by Sofiev et al. (2009) and Stein et al. (2009) in their evaluations of the European and US smoke forecasting systems, respectively. The consistency of these results suggests a general tendency for overpredictions during major fire events for these smoke emission and dispersion models. This might be partly attributed to the inability of the monitors to reliably measure such a high concentrations. Another possible explanation is related to the characteristics of modeling. Most air quality models consist of different statistical equations to compute different elements needed. For example, the total emissions of PM are calculated from emissions factors of certain fuel and the total fuel consumption. However, when applying these equations with inputs from the very intense fires, it can lead to results too large to be realistic. The available evidence suggests that very high forecast concentrations should be scaled or truncated to better reflect realistic measured concentrations.

Most of the model evaluation results suggest that the 48-hour predictions agree better with the monitor observations than the 24-hour predictions. A possible explanation for this observation is related to the dispersion of the smoke plumes. The BlueSky system we evalu-

ate does not account for the dispersed smoke predicted in the previous forecast, which means that every prediction starts from the source of fire at the very beginning of the predictions cycle. As a result, smoke predicted in the first 24 hours might be less dispersed with higher concentrations. If the trajectory of this less dispersed plume is accurately predicted, it can result in a day with very good agreement. If the trajectory of this less dispersed plume is inaccurately predicted, the concentrated smoke prediction can result in great discrepancies when comparing with the observations.

4.2 Association with health outcomes

Physician visits for asthma were significantly associated with most of the exposure metrics tested in the study. The results for a 30μg/m^3 increase in monitor-observed $PM_{2.5}$ [RR=1.07; 95% confidence interval (CI), 1.00 – 1.15] and for the presence versus absence of HMS smoke coverage (RR=1.09; CI, 1.00 – 1.18) compare well with the results from the study by Henderson et al. (2011) on the 2003 forest fires also in British Columbia, the most similar study recently published. In the Henderson et al. (2011) study, a 30-μg/m^3 increase in monitor-observed PM_{10} was associated with a 16% increase in the odds of an asthma-specific physician visit (OR = 1.16; 95% CI, 1.09–1.23) and being covered by HMS was associated with 21% increase in odds (OR=1.21; 95% CI, 1.00–1.47). Although Henderson et al. (2009) used measures of PM_{10} instead of $PM_{2.5}$ as in our study, the results can still be compared since $PM_{2.5}$ is the major fraction of PM_{10} from wildfire smoke (Moore et al., 2006, Wu et al. 2006). So far, only one study (Caamano-Isorna et al., 2011) has reported using medication dispensation as health outcome. The result from our study suggests it has similar association as asthma physician visit with the exposure metrics, even slightly more sensitive for some exposure metrics.

A 30-μg/m^3 increase in 24-hour and 48-hour BlueSky $PM_{2.5}$ predictions was associated with 1% and 4% increase in asthma physician visits. The same increase in predictions was also associated with 1% and 4% increase in medication dispensations. The relative risks of these associations were much lower when compared with those derived from monitor observations. In Henderson et al. (2011), a 60-μg/m^3 increase in $PM_{2.5}$ from forest fire modeled by CALPUFF (a retrospective model rather than a forecast) was associated with 4% increase of odds of asthma-specific physician visits (OR=1.04, 95% CI, 1.02 – 1.06). Correspondingly, a 60-μg/m^3 increase in $PM_{2.5}$ by BlueSky for 24-hour and 48-hour forecast was associated with 1% (RR=1.01; 95% CI, 1.00 – 1.03) and 8% (RR=1.08; 95% CI, 1.02 – 1.15) increase in relative risk of asthma physician visits, respectively, comparable with the CALPUFF result in Henderson et al. (2001). In both of the studies, modeled exposures had much narrower confidence intervals of OR/RR than monitor observations. These tight confidence intervals might be related to the great variability in the modeled exposures. As described Section 3.2.1, the BlueSky predictions had a much wider range compared with the monitoring measurements. Figure 4.1 compares the RRs and their confidence intervals calculated using all of the BlueSky predictions with those calculated using only the truncate of predictions smaller than 300μg/m^3, excluding the extremely large data predictions. Generally larger confidence intervals are found with the subset and the difference is more obvious in the BlueSky 24-hour predictions, which has more extreme values than the 48-hour predictions.

Another similar study by Delfino et al. (2009) found that a 30-μg/m^3 increase in $PM_{2.5}$ was associated with 5% increase in RR of asthma hospital admission (RR=1.07; 95%CI, 1.04 – 1.11). The RR of medication dispensations associated with monitor observations in this study was similar to results from Delfino et al. (2009) while other RRs were much smaller.

The extremely large values in the BlueSky predictions may be one of the reasons for this difference. As shown in Figure 4.1, RRs calculated with subset of data excluding predictions over 300μg/m^3 are larger than those calculated with all of the data. Other possible reasons include the differences in misclassification from different exposure assessment tools, as well as in the sensitivity of the different health outcome measures to detect health responses. In addition, the difference in study design and sources of data could also play a role in this variation.

The results from Table 3.4 and Figure 3.7 suggest that coverage by BlueSky plumes is associated with similar relative risk increase of the two health outcomes as covering by HMS plumes, with slightly narrower confidence intervals. This indicates that coverage of BlueSky plumes may have similar predictive power as HMS plumes.

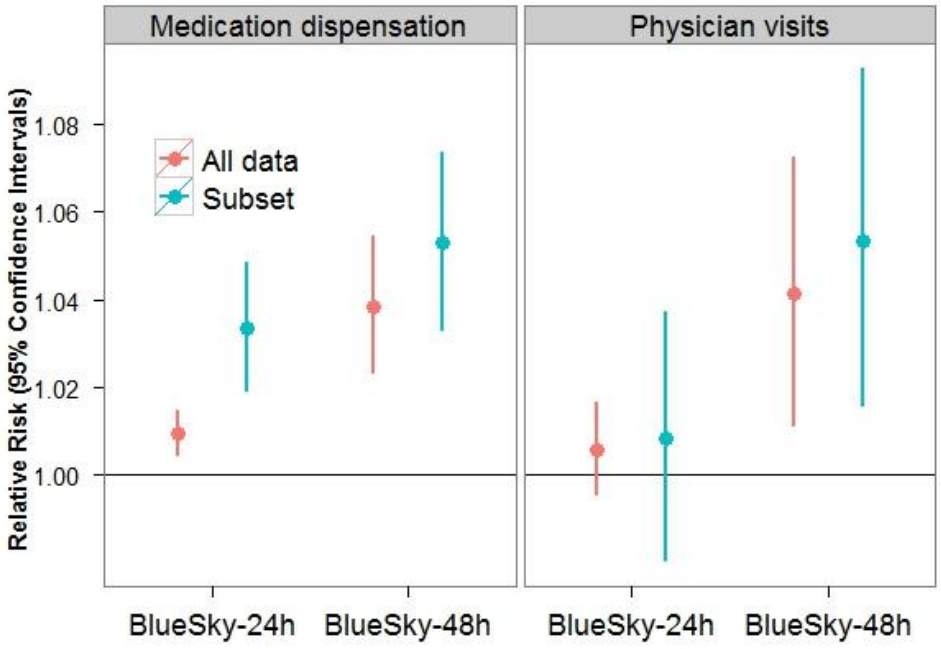

Figure 4.1 Relative risks of medication dispensations and physician visits associated with 30μg/m^3 increase in BlueSky predictions.
Point range in red indicates RRs calculated with all the data and point range in blue indicates RRs calculated with the subset of BlueSky predictions smaller than 300μg/m^3.

The BlueSky 24-hour predictions were associated with slightly smaller RRs than the BlueSky 48-hour predictions in all of the analyses. As mentioned previously in the model evaluation section, BlueSky 48-hour predictions had better overall agreement with the reference tools and its performance was more stable than the 24-hour predictions. Also, the 45-hour predictions had fewer extremely high values. Thus, BlueSky 24-hour predictions might contribute to more frequent and larger-scale exposure misclassification, driving the association towards null.

4.3 Strengths

This study is the first one to quantitatively and systematically examine the performance of the BlueSky wildfire smoke forecasting system and also the first evaluation of the Canadian version of this system. Multiple reference tools for wildfire smoke exposure assessment and a variety of statistical methods were included to provide a more comprehensive evaluation.

This is also the first study to associate wildfire smoke forecast results with respiratory health outcome indicators. Respiratory health outcome measures such as physician visits for asthma, which has the best established association with wildfire smoke exposure measurements by other studies, is a good starting point for assessing their association with smoke predictions. The results give confidence in using this prediction tool to inform actions to mitigate the adverse health effects from wildfire smoke.

Besides associating BlueSky predictions with the health outcomes, this study also associates the two reference tools, monitoring observations and HMS plume coverage, with the health outcomes. Not only does this help to compare the study results with other similar stud-

ies, but also produces the opportunity to compare relative risks resulting from different tools.

Ground-level monitoring observations and HMS satellite smoke plume images were used for the evaluation of the BlueSky predictions on different aspects. While monitoring observations can serve as a "gold standard" for absolute values of $PM_{2.5}$ concentrations, satellite images can be a good reference tool for plume sizes, shapes and locations. Satellite instruments are not physically affected by smoke or fires during intense fire periods, while monitoring stations might be out of function.

Because the study covers the whole 2010 fire season and multiple locations in British Columbia, evaluation of model predictions can be done both temporally and spatially. By doing this, we can have a better idea of when and where the system tends to have good or poor performance. A range of well-established and commonly used statistics for model evaluation was applied, providing quantitative measurements of agreement on different aspects including correlation, differences, and spatial agreement. The results from these statistically valid methods indicate that BlueSky has performed comparably with other existing wildfire smoke forecasting models.

4.4 Limitations

There are several limitations associated with this study. First, in the evaluation of the BlueSky performance, the reference tools used were not exactly the "gold standards" because what they were measuring was different from what was predicted by BlueSky. Monitor observations capture $PM_{2.5}$ from all sources while BlueSky predicts only PM coming from wildfire smoke. Because PM from wildfire smoke was extremely high compared with other sources during the major fire events at areas close to the fire origins, it was reasonable to as-

sume that the dominant source of monitor-observed $PM_{2.5}$ was from fire smoke. However, in areas where fire smoke only had mild effects, monitor observations might reflect a large fraction of PM from other sources, thus affecting the agreement with BlueSky. This is also one of the reasons why BlueSky predictions better agreed with monitor observations during specific times and at specific locations. On the other hand, HMS images detect wildfire smoke in the total column of the atmosphere, but BlueSky only predicts smoke dispersed at the ground-level. This difference might be one of the reasons why HMS smoke plumes were much larger than BlueSky predicted plumes most of the time.

Second, the BlueSky forecasting system is an ongoing research project, and changes continue to be made. As a result, this study used the predictions from 2010 fire season data that were rerun with improvements to the system implemented in 2011. In the 2012 fire season, some other changes, including incorporating a new fire information system which can clump multiple fire hotspots, were made to the system again. These changes can potentially affect the performance. Under the scope of this study, it is not possible to rerun all the data and analyses with the newly improved system. Most importantly, as research on the system continues and more changes will be implemented, additional evaluations should be conducted. This study has developed systematic methods with multiple quantitative analyses to assess the system performance on different aspects, including the spatial and temporal agreement, considering both the absolute $PM_{2.5}$ concentration predictions and the smoke plume coverage. These methods can be used in the future evaluations to assess the improvement of revised systems.

Third, limited by the scope of this study, no in-depth investigation was done on the BlueSky forecast system design. As a result, no technical advice can be drawn from this

study on possible causes for observed discrepancies. Further evaluations should be conducted on the performance of the different components of the forecasting system, such as the calculation of the PM emissions, the estimation of the plume injection height, and the performance of the meteorological forecast. However, this study provides knowledge of the general trends, such as more frequent and severe overpredictions than underpredictions, which can serve as clues for further investigation.

Fourth, health outcomes used in this study were aggregated counts based on the unit of local health area (LHA), which was quite a large geographical area. Exposure to fire smoke among populations within the same LHA can be very different, but one value was assigned to the whole LHA. This can potentially lead to exposure misclassification and drive the association results towards null.

Fifth, some potential factors that might influence the association were not included, such as the basic demographics for populations in different LHAs. This might not have a great impact on the reported association (because most of them were not changing over such a short period of time), but it might influence the assessment of the strength of the association.

Sixth, although associations were identified between fire smoke and health outcome measures, it was unclear if changes in the health outcome indicators were really driven by responses to smoke exposure. The possibility that more people were getting their medication not because they had responses to the smoke exposure but just to get prepared for the smoke events could not be ruled out.

4.5 Future work

As mentioned before, the BlueSky system is an ongoing project and great efforts have been made to improve its performance. Thus, evaluation of the model predictions should be continued in the future as the system develops, helping to ensure their robustness. Other tools for wildfire smoke exposure assessment, such as MODIS detected aerosol optical depth (AOD), can also be included as references in future studies. As it is impossible to find a single perfect gold standard, including more tools as references might provide a better and more comprehensive evaluation.

Other health outcome indicators, such as hospital admission, can also be associated with BlueSky predictions. As mentioned previously, the ultimate goal for associating smoke measurement and predictions with health outcomes is to mitigate the impact of wildfire smoke on public health. Thus, more research on establishing an applicable tool for decision making based on these results, using multiple resources, should be conducted. Ideally, a tool that can provide quantitative information, such as thresholds of PM predictions for taking certain public health actions, with an implication of the magnitude health impact that can be achieved by these actions.

4.6 Conclusions

The objectives of this thesis study have been realized: a systematic and quantitative evaluation of the BlueSky smoke forecasting system has been conducted and associations between BlueSky predictions and health outcome measures have been found. The evaluation found that agreement between BlueSky predictions and monitoring as well as remote sensing data was reasonable compared with evaluations of other existing smoke forecasting systems.

Good agreement was generally observed during intense fire periods and in areas heavily and consistently impacted by fire smoke. Overall, BlueSky predicts smaller plumes than HMS images but higher concentrations of $PM_{2.5}$ than monitoring observations during intensive smoky days. Significant relative risks of respiratory health outcomes were found associated with BlueSky predictions, and the risks were consistent with those for the reference tools and those reported by other epidemiological studies.

The results of this study suggest that the BlueSky smoke forecasting system produces reasonably useful predictions of PM related to wildfire smoke, and those predictions can be valuable for public health applications.

References

Airfire, US Forest Service. (2010) BlueSky Framework. Retrieved on August 18, 2011 from http://airfire.org/bluesky

Air Resources Laboratory (ARL). (2011) HYSPLIT - Hybrid Single Particle Lagrangian Integrated Trajectory Model. Retrieved on February 23, 2012 from http://www.arl.noaa.gov/HYSPLIT_info.php

Altman, D. G., & Bland, J. M. (1983). Measurement in Medicine: The Analysis of Method Comparison Studies. The Statistician, 32(3): 307

Andreae, M. O., & Merlet, P. (2001) Emission of trace gases and aerosols from biomass burning. Global Biogeochemical Cycles, 15(4): 955-966

B.C. Ministry of Forests, Mines and Lands (2010) The State of British Columbia's Forests, 3rd ed. Forest Practices and Investment Branch, Victoria, B.C. Retrieved on August 28, 2012 www.for.gov.bc.ca/hfp/sof/index.htm#2010_report

BC Stats (2009) Metadata information: Local health area boundaries. Retrieved on July 29, 2012 https://apps.gov.bc.ca/pub/geometadata/metadataDetail.do?recordUID=49698&recordSet=ISO19115

British Columbia Forest Service, Wildfire Management Branch. Fire Locations 2010. Accessed April 21, 2011 http://bcwildfire.ca/History/LargeFires2010.htm

Caamano-Isorna, F., Figueiras, A., Sastre, I., Montes-Martínez, A., Margarita Taracido, & Piñeiro-Lamas, M. (2011) Respiratory and mental health effects of wildfires: an ecological study in Galician municipalities (north-west Spain). Environmental Health, 10(1): 48. doi:10.1186/1476-069X-10-48

Damoah, R., Spichtinger, N., Forster, C., James, P., Mattis, I., Wandinger, U., . . . Stohl, A.(2004) Around the world in 17 days - hemispheric-scale transport of forest fire smoke from Russia in May 2003. Atmospheric Chemistry and Physics, 4: 1311-1321

Danielsen P.H., Loft S., Kocbach A., Schwarze P.E., & Moller P. (2009) Oxidative damage to DNA and repair induced by Norwegian wood smoke particles in human A549 and THP-1 cell lines. Mutation Research/Genetic Toxicology and Environmental Mutagenesis, 674 (1-2): 116-122.

De Kok, T.M.C.M., Driece, H.A.L., Hogervorst, J.G.F., & Briede, J.J. (2006) Toxicological assessment of ambient and traffic-related particulate matter: A review of recent studies. Mutation Research, 613: 103–122

Delfino,R.J., Brummel,S., Wu,J., Stern,H., Ostro,B., Lipsett,M., . . . Gillen,D.L. (2009) The relationship of respiratory and cardiovascular hospital admissions to the southern California wildfires of 2003. Occupational and Environmental Medicine, 66:189–197

Dennekamp, M., & Abramson, M. J. (2011) The effects of bushfire smoke on respiratory health. Respirology, 16: 198–209

Dirksen, R. J., Boersma, K. F., de Laat, J., Stammes, P., van der Werf, G. R., Val Martin, M., & Kelder, H. M. (2009) An aerosol boomerang: Rapid around-the-world transport of smoke from the December 2006 Australian forest fires observed from space. Journal of Geophysical Research, 114: D21201

Fiebig, M., Petzold, A., Wandinger, U., Wendisch, M., Kiemle, C., Stifter, A., . . . Leiterer, U. (2002) Optical closure for an aerosol column: Method, accuracy, and inferable properties applied to a biomass-burning aerosol and its radiative forcing, Journal of Geophysical Research, 107(D21): 8130

Fire and Environmental Research Application Team (FERA) (2011) CONSUME. Retrieved on February 22, 2012 from http://www.fs.fed.us/pnw/fera/research/smoke/consume/index.shtml

Flannigan, M.D., & Van Wagner, C.E. (1991) Climate change and wildfire in Canada. Canadian Journal of Forest Research, 21(10): 66-72

Forchhammer,L., Loft,S., Roursgaard, M., Cao, Y., Riddervold,I.S., Sigsgaard,T., & Møller,P. (2012) Expression of adhesion molecules, monocyte interactions and oxidative stress in human endothelial cells exposed to wood smoke and diesel exhaust particulate matter. Toxicology Letters, 209(2): 121-128

Formenti, P., Reiner, T., Sprung, D., Andreae, M.O., Wendisch, M., Wex, H., . . . Zerefos, C. (2002), STAAARTE-MED 1998 summer airborne measurements over the Aegean Sea 1. Aerosol particles and trace gases, Journal of Geophysical Research, 107(D21): 4550

Giglio, L., Descloitres, J., Justice, C. O., & Kaufman, Y. J. (2003). An Enhanced Contextual Fire Detection Algorithm for MODIS. Remote Sensing of Environment, 87(2-3): 273-282

Government of Canada. (2010) Wildfires in Canada: wildfire facts. Retrieved April 6, 2012 http://www.getprepared.gc.ca/knw/ris/wldf-eng.aspx

Hanigan, I.C., Johnston, F.H., & Morgan, G.G. (2008) Vegetation fire smoke, indigenous status and cardio-respiratory hospital admissions in Darwin, Australia, 1996–2005: a time-series study. Environmental Health, 7:42

Henderson, S.B., Brauer, M., MacNab, Y.C., & Kennedy, S.M. (2011) Three Measures of Forest Fire Smoke Exposure and Their Associations with Respiratory and Cardiovascular Health Outcomes in a Population-Based Cohort. Environmental Health Perspective:-. doi:10.1289/ehp.1002288

Henderson, S.B., & Johnston, F.H. (2012) Measures of forest fire smoke exposure and their associations with respiratory health outcomes. Current opinion in allergy and clinical immunology, 12(3): 221–227. doi:10.1097/ACI.0b013e328353351f

Holstius, D,M,, Reid, C.E., Jesdale, B.M., & Morello-Frosch, R. (2012) Birth Weight Following Pregnancy During the 2003 Southern California Wildfires. Environmental Health Perspective, http://dx.doi.org/10.1289/ehp.1104515

Hsu, N. C., Herman, J. R., Gleason, J. F., Torres, O., & Seftor, C. J. (1999) Satellite detection of smoke aerosols over a snow/ice surface by TOMS. Geophysical Research Letter, 26(8): 1165–1168

Hueglin, C.H., Gaegauf, C.H., Künzel, S., & Burtscher, H. (1997) Characterization of Wood Combustion Particles: Morphology, Mobility, and Photoelectric Activity. Environmental Science and Technology, 31: 3439-3447

Ichoku, C., & Kaufman, J.Y. (2005) A Method to Derive Smoke Emission Rates From MODIS Fire Radiative Energy Measurements, IEEE Transactions on Geoscience and Remote Sensing, 43 (11): 2636- 2649

Jalava, P. I., Salonen, R. O., Hälinen, A. I., Penttinen, P., Pennanen, A. S., Sillanpää, M., Sandell, E.,…Hirvonen, M. (2006) In vitro inflammatory and cytotoxic effects of size-segregated particulate samples collected during long-range transport of wildfire smoke to Helsinki. Toxicology and Applied Pharmacology, 215(3): 341–353.

Johnston, F.H., Bailie, R.S., Pilotto, L.S., & Hanigan, I.C. (2007) Ambient biomass smoke and cardio-respiratory hospital admissions in Darwin, Australia. BMC Public Health, 7: 240

Johnston, F.H., Henderson, S.B., Chen, Y., Randerson, J.T., Marlier, M., . . . Brauer, M. (2012) Estimated Global Mortality Attributable to Smoke from Landscape Fires. Environmental Health Perspective, doi:10.1289/ehp.1104422

Karlsson, H.L., Ljungman, A.G., Lindbom, J., & Moller, L. (2006) Comparison of genotoxic and inflammatory effects of particles generated by wood combustion, a road simulator and collected from street and subway. Toxicology Letter, 165: 203–211

Keane, J.C. (2012) Air quality and visibility in Southwestern British Columbia during forest fire smoke events. Unpublished master's thesis, University of British Columbia, Vancouver, Canada.

Klikach, V. (2011) Final report. Alberta Envrionment (unpublished)

Kocbach, A., Namork, E., & Schwarze, P. E. (2008a) Pro-inflammatory potential of wood smoke and traffic-derived particles in a monocytic cell line. Toxicology, 247(2–3): 123-132

Kocbach A., Herseth J.I., Lag M., Refsnes M., & Schwarze P.E. (2008b) Particles from wood smoke and traffic induce differential pro-inflammatory response patterns in co-cultures Toxicology and Applied Pharmacology, 232 (2): 317-326.

Kochi, I., Donovan, G.H., Champ, P.A., & Loomis, J.B. (2010) The economic cost of adverse health effects from wildfire-smoke exposure: a review International Journal of Wildland Fire, 19:803–817

Kubátová, A., Steckler, T. S., Gallagher, J. R., Hawthorne, S. B., & Picklo, M. J. (2004) Toxicity of wide-range polarity fractions from wood smoke and diesel exhaust particulate obtained using hot pressurized water. Environmental Toxicology and Chemistry, 23: 2243–2250

Kurz, W. A., Dymond, C. C., Stinson, G., Rampley, G. J., Neilson, E. T., Carroll, A. L., . . . Safranyik, L. (2008) Mountain pine beetle and forest carbon feedback to climate change. Nature, 452(7190): 987–990.

Lakshmanan, C.M. & Hoelscher, H.E. (1970) Production of Levoglucosan by Pyrolysis of Carbohydrates. Pyrolysis in Hot Inert Gas Stream. Industrial & Engineering Chemistry Product Research and Development 9: 57. doi:10.1021/i360033a011

Larkin, N.K., O'Neil, S.M., Solomon, R., Raffuse, S., Strand, T., Sullivan, D.C., . . . Ferguson, S.A. (2009) The BlueSky smoke modeling framework. International Journal of Wildland Fire, 18: 906-920

Lee, K.H., Li, Z., Kim, Y.L., &Kokhanovsky, A.A. (2009) Aerosol monitoring from satellite observations: a history of three decades. In Y.J. Kim, U. Platt, M.B. Gu & H. Iwahashi (Eds.), Atmospheric and Biological Environmental Monitoring (pp.13-38). Berlin, Germany: Springer

Lee, T.S., Falter,K., Meyer,P., Mott,J., & Gwynn,C. (2009) Risk factors associated with clinic visits during the 1999 forest fires near the Hoopa Valley Indian Reservation, California, USA. International Journal of Environmental Health Research, 19(5): 315-327

Leithead, A., Li, S., Hoff, R., Cheng, Y., Brook, J. (2006) Levoglucosan and dehydroabietic acid: Evidence of biomass burning impact on aerosols in the Lower Fraser Valley. Atmospheric Environment, 40 (15): 2721-2734

Li, Z., Nadon, S., & Cihlar, J. (2000) Satellite-based detection of Canadian boreal forest fires: Development and application of the algorithm. International Journal of Remote Sensing, 21(16): 3057-3069

Lin, S., Luo, M., Walker, R.J., Liu, X., Hwang, S.A., & Chinery, R. (2009) Extreme high temperatures and hospital admissions for respiratory and cardiovascular diseases. Epidemiology, 20 (5): 738-46

Michelozzi, P., Accetta, G., De Sario, M., D'Ippoliti, D., Marino, C., Baccini, M.,…Perucci, C.A. (2009) High Temperature and Hospitalizations for Cardiovascular and Respiratory Causes in 12 European Cities. Amerian Journal of Respiratory and Critical Care Medicine, 179: 383-389

Migliaccio, C., & Mauderly, J. (2010) Biomass smoke exposures: toxicology and animal study design. Inhalation Toxicology, 22(2), 104-107.

Moore, D., Copes, R., Fisk, R., Joy, R., Chan, K., & Brauer, M. (2006) Population health effects of air quality changes due to forest fires in British Columbia in 2003 - Estimates from physician-visit billing data. Canadian Journal of Public Health, 97(2): 105-108

Morgan, G., Sheppeard, V., Khalaj, B., Ayyar, A., Lincoln, D., Jalaludin, B., . . . Lumley, T. (2010) Effects of bushfire smoke on daily mortality and hospital admissions in Sydney, Australia. Epidemiology, 21: 47–55.

Mosca, S., Graziani, G., Klug, W., Bellasio, P., & Bianconi, R. (1998) A statistical methodology for the evaluation of long-range dispersion models: an application to the ETEX exercise. Atmospheric Environment, 32(24): 4307-4324

NASA (2012) MODIS web: about MODIS. Retrieved on September 25, 2012 from http://modis.gsfc.nasa.gov/about/

Natural Resources Canada. (2011) Canadian Wildland Fire Information System: Background Information. Retrieved on January 10, 2012 from http://cwfis.cfs.nrcan.gc.ca/en_CA/background

Naeher,L.P., Brauer,M., Lipsett,M., Zelikoff, J.T., Simpson,C.D., Koenig,J.Q., & Smith,K.R. (2007) Woodsmoke health effects: a review. Inhalation Toxicology, 19: 67-106

National Center for Environmental Prediction. (2012a) Environmental Modeling Center: NAM. Retrieved on February 22, 2012 from http://www.emc.ncep.noaa.gov/?branch=NAM

National Center for Environmental Prediction. (2012b) Environmental Modeling Center: GFS. Retrieved on February 22, 2012 from http://www.emc.ncep.noaa.gov/GFS/

National Oceanic and Atmospheric Administration (NOAA) (2011) Hazard Mapping System Fire and Smoke Product. Retrieved on August 17, 2011 from http://www.osdpd.noaa.gov/ml/land/hms.html

National Wildfire Coordinating Group (2002) Gaining A Basic Understanding of the National Fire Danger Rating System. Retrieved on February 22, 2012 from http://geology.isu.edu/geostac/Field_Exercise/wildfire/images/Basic_NFDRS.pdf

Okuda,T., Kumata,H., Zakaria,M.P., Naraoka,H., Ishiwatari,R., & Takada,H. (2002) Source identification of Malaysian atmospheric polycyclic aromatic hydrocarbons nearby forest fires using molecular and isotopic compositions. Atmospheric Environment, 36(4): 611-618

Page, W. G., Jenkins, M. J., & Runyon, J. B. (2012) Mountain pine beetle attack alters the chemistry and flammability of lodgepole pine foliage. Canadian Journal of Forest Research, 42(8): 1631–1647.

Pio,C.A., Legrand, M., Alves, C.A., Oliveira, T., Afonso, J., Caseiro, A., . . . Gelencsér, A. (2008) Chemical composition of atmospheric aerosols during the 2003 summer intense forest fire period. Atmospheric Environment, 42(32):7530-7543

Prins, E.M. & Menzel, M.P. (1992) Geostationary satellite detection of biomass burning in South America. International Journal of Remote Sensing, 13(15): 2783-2799

Province of British Columbia. (2011) Summary of previous fire seasons: 2010 fire season. Retrieved on July 23, 2012 from http://bcwildfire.ca/History/SummaryArchive.htm#2010

Phuleria, H. C., Fine, P. M., Zhu, Y., & Sioutas, C. (2005) Air quality impacts of the October 2003 Southern California wildfires. Journal of Geophysical Research, 110, D07S20, doi:10.1029/2004JD004626.

Rappold, A.G., Stone, S.L., Cascio, W.E., Neas, L.M., Kilaru, V.J., Carraway, M.S., . . . Deyneka, L. (2011) Peat Bog Wildfire Smoke Exposure in Rural North Carolina Is Associated with Cardio-Pulmonary Emergency Department Visits Assessed Through Syndromic Surveillance. Environmental Health Perspective:-. doi:10.1289/ehp.1003206

Reid, J. S., Koppmann, R., Eck, T. F., & Eleuterio, D. P. (2005) A review of biomass burning emissions part II: intensive physical properties of biomass burning particles. Atmospheric Chemistry and Physics, 5: 799-825

Rolph, G.D., Draxler, R. R., Stein, A.F., Taylor, A., Ruminski, M.G., Kondragunta, S., . . . Davidson, P.M. (2009) Description and Verification of the NOAA Smoke Forecasting System: The 2007 Fire Season. Weather and Forecasting, 24: 361-378

Ruminski,M., Kondragunta,S., Draxler,R., & Zeng,J. (2006, May) Recent Changes to the Hazard Mapping System. 15th International Emission Inventory Conference, New Orleans, Louisiana

Saarnio,K., Aurela,M., Timonen,H., Saarikoski,S., Teinilä,K., Mäkelä,T., . . . Hillamo,R. (2010) Chemical composition of fine particles in fresh smoke plumes from boreal wildland fires in Europe. Science of the Total Environment, 408(12): 2527-2542

Sakiyama, S. (2011) The BlueSky Western Canada Wildfire Smoke Forecasting System. Retrieved on August 18, 2011 from http://www.bcairquality.ca/bluesky/

Samsonov, Y. N., Belenko, O. A., & Ivanov, V. A. (2010) Dispersal and morphological characteristics of smoke particulate emission from fires in the boreal forests of Siberia. Atmospheric and Oceanic Optics, 23(6), 485-493

Samuelsen M., Nygaard U.C., & Lovik M. (2008) Allergy adjuvant effect of particles from wood smoke and road traffic. Toxicology, 246 (2-3): 124-131.

Sapkota, A., Symons, J.M., Kleissl, J., Wang, L., Parlange, M.B., Ondov, J., . . . Buckley, T.J. (2005) Impact of the 2002 Canadian Forest Fires on Particulate Matter Air Quality in Baltimore City. Environmental Science & Technology, 39 (1): 24-32

Schowengerdt, R.A. (2007) Remote sensing: models and methods for image processing (3rd ed.). Burlington, MA: Academic Press.

Schranz, C.I., Castillo,E.M., & Vilke,G.M. (2010) The 2007 San Diego Wildfire Impact on the Emergency Department of the University of California, San Diego Hospital System. Prehospital and Disaster Medicine, 25(5): 472-476

Sillanpää, M., Saarikoskia, S., Hillamoa, R., Pennanenb, A., Makkonena, U., Spolnikc, Z., . . . Salonen, R.O. (2005) Chemical composition, mass size distribution and source analysis of long-range transported wildfire smokes in Helsinki. Science of the Total Environment, 350: 119– 135

Sofiev, M., Vankevich, R., Lotjonen, M., Prank, M., Petukhov, V., Ermakova, T., . . . Kukkonen, J.: An operational system for the assimilation of the satellite information on wild-land fires for the needs of air quality modelling and forecasting, Atmos. Chem. Phys., 9, 6833-6847

Stocks, B.J., Mason, J.A., Todd, J.B., Bosch, E.M., Wotton, B.M., Amiro, B.D., . . . Skinner, W.R. (2002) Large forest fires in Canada, 1959–1997. Journal of Geophysical Research, 107, 8149

Swiston, J. R., Davidson, W., Attridge, S., Li, G. T., Brauer, M., & van Eeden, S. F. (2008) Wood smoke exposure induces a pulmonary and systemic inflammatory response in firefighters. European Respiratory Journal, 32:129-138

Tan, W.C., Qiu, D., Liam, B.L., Ng, T.P., Lee, S.H., van Eeden, S.F., . . . Hogg, J.C. (2000) The human bone marrow response to acute air pollution caused by forest fires. American Journal of Respiratory and Critical Care Medicine, 161(4 Pt 1):1213-7

Taylor, E., Kellerhals, M., Sakiyama, S., & Coccola, C. (2012) Estimating the Air Quality Health Index during Wildfire Smoke Events in the BC Interior Using Visibility Measurements. Report available from Air Protection Section, Ministry of Environment, Victoria, British Columbia

Tham, R., Erbas, B., Akram, M., Dennekamp, M. & Abramson, M. J. (2009) The impact of smoke on respiratory hospital outcomes during the 2002–2003 bushfire season, Victoria, Australia. Respirology, 14: 69–75

Tikuisis, P., Kane, D.M., McLellan, T.M., Buick, F., & Fairburn, S.M. (1992) Rate of formation of carboxyhemoglobin in exercising humans exposed to carbon monoxide. Journal of Applied Physiology 72 (4): 1311–9

University Corporation for Atmospheric Research (UCAR). (2008) MM5 community model. Retrieved on January 13th, 2012 from http://www.mmm.ucar.edu/mm5/

van Eeden, S.F., Tan, W.C., Suwa, T., Mukae, H., Terashima, T., Fujii, T., . . . Hogg ,J.C. (2001) Cytokines involved in the systemic inflammatory response induced by exposure to particulate matter air pollutants (PM(10)). American Journal of Respiratory and Critical Care Medicine, 164(5):826-30

Vedal,S., & Dutton,S.J. (2006) Wildfire air pollution and daily mortality in a large urban area. Environmental Research, 102: 29-35

Veronesi, B., Haar, C., Lee, L., & Oortgiesen, M. (2002) The surface charge of visible particulate matter predicts biological activation in human bronchial epithelial cells. Toxicology and Applied Pharmacology, 178: 144–154.

Viswanathan, S., Eria,L., Diunugala,N., Johnson,J., & McClean,C. (2006) An Analysis of Effects of San Diego Wildfire on Ambient Air Quality. Journal of Air & Waste Management Association, 56: 56–67

Wandinger, U., Müller, D., Böckmann, C., Althausen, D., Matthias, V., Bösenberg, J., . . . Ansmann, A. (2002) Optical and microphysical characterization of biomass-burning and industrial-pollution aerosols from multiwavelength lidar and aircraft measurements. Journal of Geophysical Research, 107, 8125

Warner, S., Platt, N., & Heagy, J.F. (2004) User-Oriented Two-Dimensional Measure of Effectiveness for the Evaluation of Transport and Dispersion Models. Journal of Applied Meteorology, 43: 58-72

Weinhold, B. (2008) Ozone nation: EPA standard panned by the people. Environmental Health Perspective, 116 (7): A302–A305

Westerling, A. L., Hidalgo, H. G., Cayan, D. R., & Swetnam, T. W. (2006) Warming and Earlier Spring Increase Western U.S. Forest Wildfire Activity. Science, 313:940-943

Wegesser, T.C., Pinkerton, K.E., & Last, J.A. (2009) California Wildfires of 2008: Coarse and Fine Particulate Matter Toxicity. Environmental Health Perspectives, 117(6): 893–897. doi:10.1289/ehp.0800166

Wotawa, G. & Trainer, M. (2000) The influence of Canadian forest fires on pollutant concentrations in the United States. Science, 288: 324–328

Wotton, B.M., Nock, C.A., & Flannigan, M.D. (2010) Forest fire occurrence and climate change in Canada. International Journal of Wildland Fire, 19: 253–271.

Wu, J., Winera, A.M., & Delfino, R.J. (2006) Exposure assessment of particulate matter air pollution before, during, and after the 2003 Southern California wildfires. Atmospheric Environment, 40: 3333–3348

Appendices

Appendix A Python and R scripts for BlueSky data preparation

A.1 Python scripts for converting NetCDF files of BlueSky outputs to csv files

```
import os
import csv

# function to dump the nc file to a text file
def dump_nc(infile):
    PMvar = 'PM25' # variable for PM infromation = PM25
    Tvar = 'TFLAG' # variable for Time flags = TFLAG
    ncdump = 'C:/Users/ayao/Documents/ncdump/ncdump -v ' + PMvar # make text string of
the command necessary to dump the .nc file
    textfile = infile.strip('.nc')+'.txt'  # name of the file to dump to = name of file to be dumped
+ .txt instead of .nc
    command = ncdump+' '+infile+' > '+textfile # create string variable of the whole command
    os.system(command) # send the command to the OS
    print infile+' has been dumped to text'

# Function pulls the 60 hours of values out of the ugly .text files in a single vector
def get_values (infile):
    dump_nc(infile)
    textfile = infile.strip('.nc')+'.txt'
    f = open(textfile, 'r') # open a channel to the ascii file output by the dump
    values = [] # empty list to be populated with all values
    count = 0 # count the number of lines read so that we can skip the first
    for line in f.readlines():
        count = count + 1
        line = line.strip()
        if count <= 55:
            continue
        else:
            line = line.split(',')
            for element in line:
                element = element.strip()
                element = element.strip(' ;') # strips the semicolon after the final zero
                element = element.strip('}') # strips the curly brace at the very end
                if element != '': # if the values isn't empty
                    values.append(round(float(element),2))
    print 'Values from '+infile+' have been collected'
    return values

# Function converts vector to matrix-ready .csv format for further manipulation in R
```

```
def write_values (infile, outfile):
    vector = get_values(infile)
    if len(vector) == 6645060:
        print 'Length of collected data is correct'
    os.remove(infile.strip('.nc')+'.txt')
    matrix = []
    for i in range(0, len(vector), 551): #create a stack of rows 601 colums wide
        matrix.append(vector[i:i+551])
    csvfile = csv.writer(open(outfile, 'wb'), delimiter = ',')
    for row in (range(len(matrix),0,-1)):
        csvfile.writerow(matrix[row-1])
    print outfile+' was written'
################################################################################
date = '26jul2010'
infile = 'C:/Users/ayao/Documents/sorted_data/2010rerun/'+date+'/'+date+'.nc'
outfile = infile.strip('.nc')+'.csv'
write_values(infile, outfile)
```

A.2 R scripts for splitting the csv files into 60 ASCII files of hourly predictions and calculating the daily averages.

```
# function to import all of the pm data from the .csv file
import_data = function(smokedate){
  smokefile = paste(basefolder, smokedate, '/', smokedate, '.csv', sep = "")
  pm = read.table(smokefile, sep = ",", header = F)
  assign("pm", pm, envir = .GlobalEnv)
  }

# function to get the hour in the file as PDT
get_hours = function(smokedate){

  filedate = as.Date(smokedate, "%d%b%Y") # get the dates of data in the file
  filedate = as.POSIXlt(filedate)

        hours = rep(filedate, 201)# get the hours in PDT  (UTC - 7 hours) Note this is currently PDT because we are *in* PDT...need to fix at a later date
        for (i in 1:59){
    filedate = filedate + 3600
    hours = c(hours, rep(filedate, 201))
                        }
                        hours = as.character(hours)
  return(hours)
  }

# function to output the hourly files
```

```
hourly_output = function(smokedate){
  hours = get_hours(smokedate) # get the vector of hours
  for (hour in unique(hours)){ # for every hour in the file output an arc ascii
    hourdata = pm[hours == hour,] # select data for the hour from the overall pm file
    headerdata = c("ncols 551", "nrows 201", "xllcorner -145", "yllcorner 45", "cellsize 0.1",
"nodata_value -999.9") # header for the ASCII raster file
    outfile = paste(basefolder, # make a sensible file name
                smokedate, "/",
                substr(hour,1,10), '_', substr(hour,12,13), '00.txt', sep = "")
    write(headerdata, outfile, sep = "/t")
    write.table(hourdata, outfile, sep = " ", row.names = F, col.names = F, append = T)
    }
   }

# get averages for the two complete calendar days (PDT) in the file
daily_output = function(smokedate){
  firstday = as.Date(smokedate, "%d%b%Y")
  secondday = firstday+1
  day1 = make24hourAv(pm, 1)
  headerdata = c("ncols 551", "nrows 201", "xllcorner -145", "yllcorner 45", "cellsize 0.1",
"nodata_value -999.9")
  outfile1 = paste(basefolder, # make a sensible file name
              smokedate, "/", firstday, '_average.txt', sep = "")
        write(headerdata, outfile1, sep = "/t")
        write.table(day1, outfile1, sep = " ", row.names = F, col.names = F, append = T)
        day2 = make24hourAv(pm, 2)
  outfile2 = paste(basefolder, # make a sensible file name
              smokedate, "/", secondday, '_average.txt', sep = "")
        write(headerdata, outfile2, sep = "/t")
        write.table(day2, outfile2, sep = " ", row.names = F, col.names = F, append = T)
  }

# a function that takes the data table and calculates the 24-hour average
make24hourAv = function(pm, day){
    hours = c()
                starthour = -7
                for (i in 1:60){
                        hours = c(hours, rep(starthour, 201))
                        starthour = starthour + 1
                        }
                        if (day == 1) {rows = which(hours == 0)}
                        if (day == 2) {rows = which(hours == 24)}
                        pm24 = matrix(0,201,551) # create an empty matrix for the 24-hour
average values
    count = 0 # for every row in the domain get the 24-hour average
                        for (rowi in rows){
```

```
                                count = count + 1
                                rowmean = pm[seq(rowi,(day*24*201),201),] # select the 24
rows needed and get first row for all 24 hours
                                pm24[count,] = as.numeric(apply(rowmean, 2, mean))
                                }
                        pm24 = round(pm24,2)
                        return(pm24)
                }
################################################################################
source("C:/Users/ayao/Documents/work_documents/bluesky_functions.r")
basefolder='C:/Users/ayao/Documents/sorted_data/2010rerun/'
smokedate = '26jul2010'
import_data(smokedate)
hourly_output(smokedate)
daily_output(smokedate
```

Appendix B R script example for the Poisson regression model.

```
# dat is the dataframe with all the exposure variables, health outcome variables and covari-
ates for all LHA and all days)
# Order the dataset with LHA IDs.
LHA=order(as.integer(dat$LHA_ID))
dat <- dat[LHA,]
# Fit the Poisson regression model using Generalized Estimation Equation (package gee in R)
fit=gee(dat$outcome~offset(log(dat$population))
        +dat$exposure
        +factor(dat$week)
        +dat$temperature
        +dat$holiday
        +factor(dat$number_of_week),
        id=dat$LHA_ID, family=poisson, corstr = "exchangeable")
summary(fit)
b = as.numeric(fit$coeff[2]*30)
   se = summary(fit)$coeff[2,2]*30
   rr = exp(b)
   lci = exp(b- 1.96*se)
   uci = exp(b+ 1.96*se)
```